Persistent Sputtering Yield Reduction in Plasma-Infused Materials

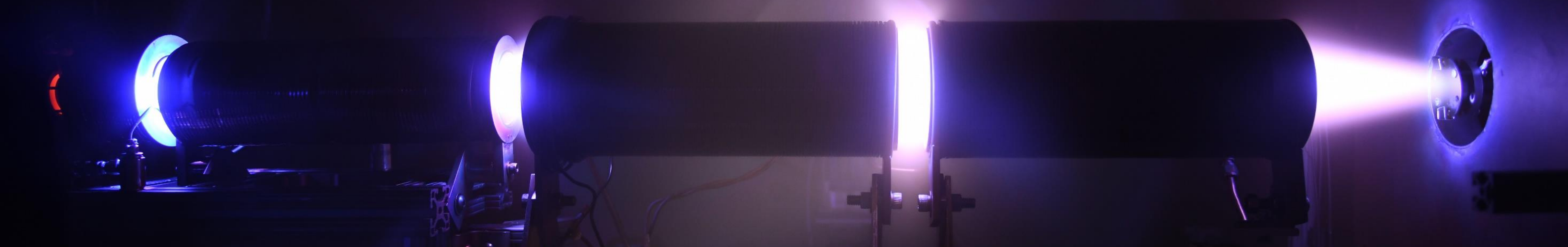

Prof. Richard Wirz
UCLA, Aerospace & Mechanical Engineering
Director, Plasma & Space Propulsion Lab
Director, Energy Innovation Lab

MIPSE
International Online Plasma Seminar (IOPS)
March 25, 2021

UCLA
PLASMA & SPACE PROPULSION LABORATORY

UCLA Plasma & Space Propulsion Laboratory

Plasma Technology

Electric Propulsion, Plasma Devices, Cathodes, Fusion

Plasma-Material Interactions (PMI)

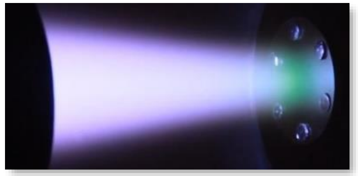

Applied Plasma Science

Plasma Control/Confinement

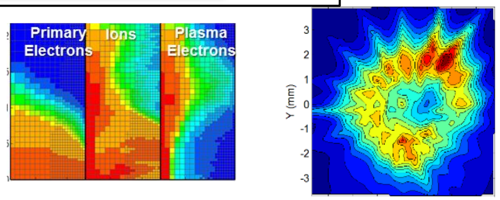

i-SEE/e-SEE
i-n
e-transport

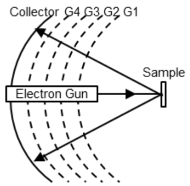

Plasma Physics

Canonical Experiments for Plasma Model Validation

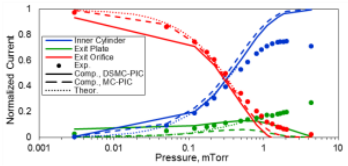

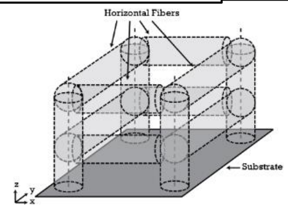

Plasma-Metamaterial Interactions (PMMI)

Uchizono N.M., Samples S.A., Wirz R.E.,

"Tunable reflectionless absorption of electromagnetic waves in a plasma–metamaterial composite structure," *Plasma Sources Sci. Technol.* 29 (2020) 085009 (5pp) https://doi.org/10.1088/1361-6595/aba489

Major Accomplishment:

Demonstrated **plasma-functionalized metamaterials** via surface wave interactions (shown on this slide)

Future Applications and Research:

1. Active protection for sensitive electronics
2. Plasma-tunable bandpass switching and protection

Discovery:

Plasma-functionalized metamaterial

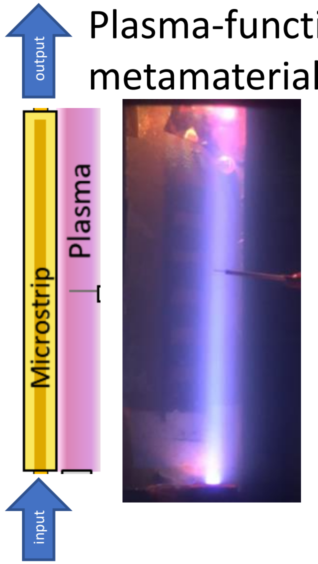

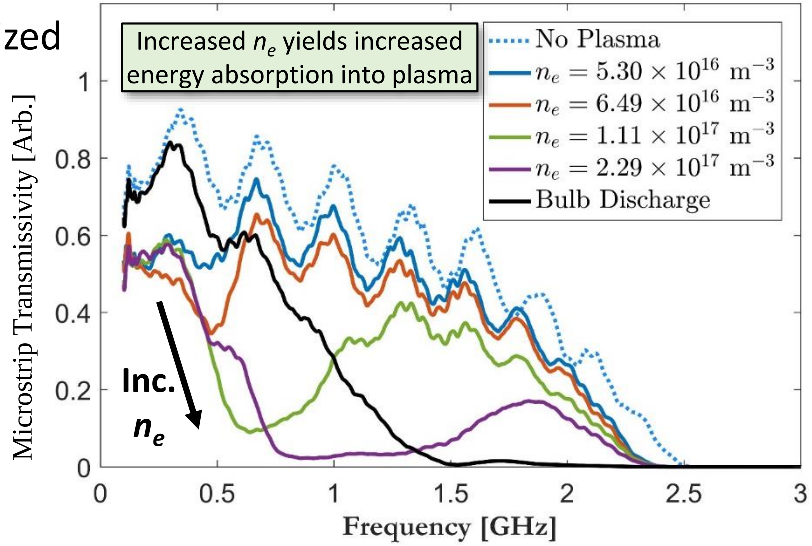

Understanding: Energy absorption caused by spoof surface plasmon (Spoof-SP) excitation of plasma surface waves (Plasma-SW)

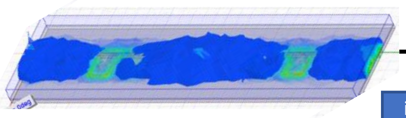

Microstrip-induced Spoof-SPs

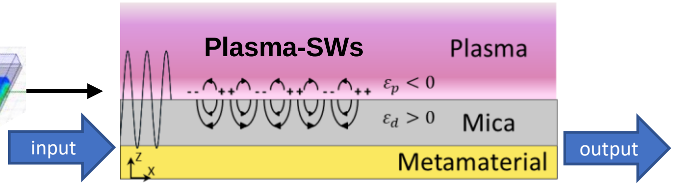

Implementation: Tunable plasma bandpass switch

Uses "reciprocal-coupling" of Spoof-SP → Plasma-SW → Spoof-SP

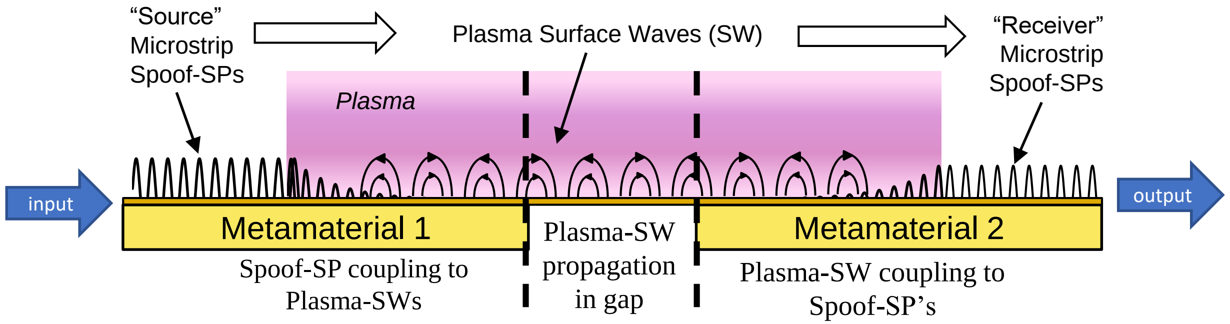

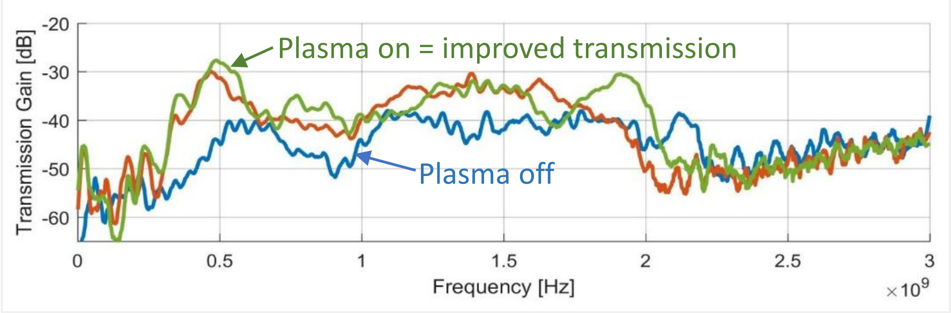

Sputtering Yield for Complex Surfaces and Materials

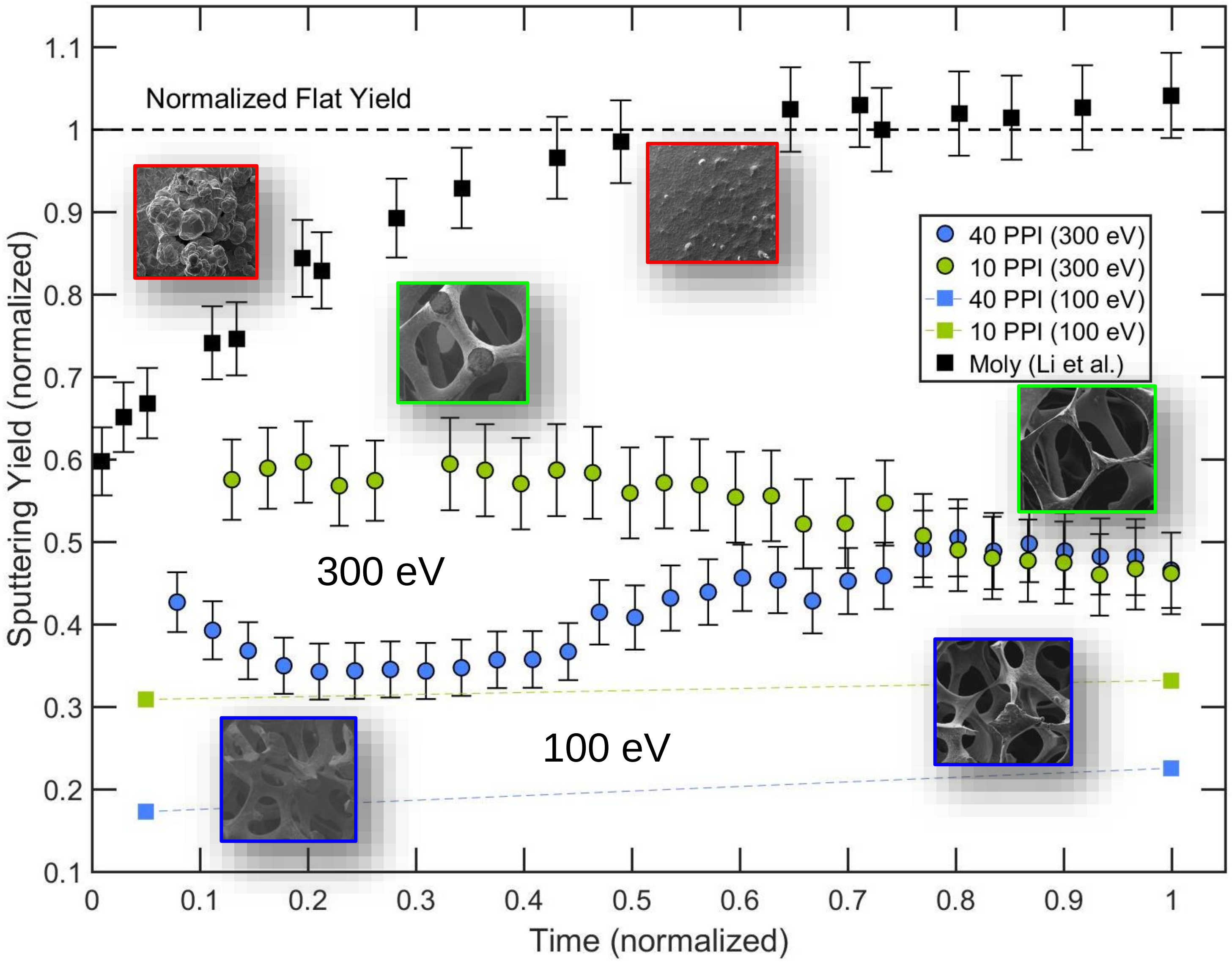

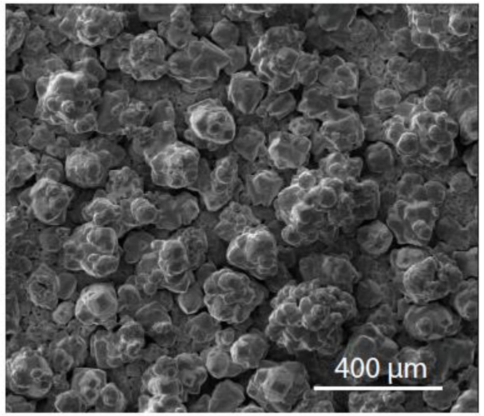

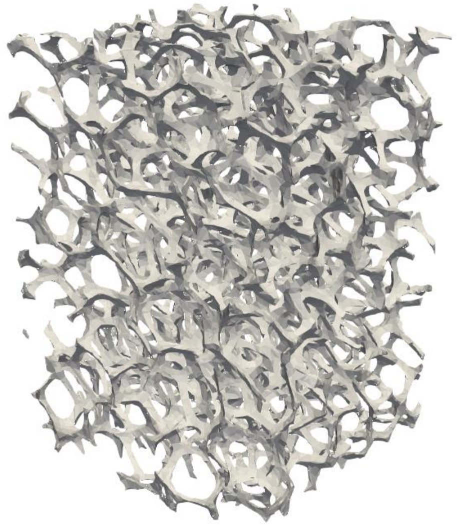

Li G., Wirz R.E., "Persistent Sputtering Yield Reduction in Plasma-Infused Foams," *Physical Review Letters*, 126 (3), 035001 (2021) https://doi.org/10.1103/PhysRevLett.126.035001

PMI Lab Members/Contributors

Dr. Marlene Patino

Dr. Chris Dodson

Dr. Cesar Huerta

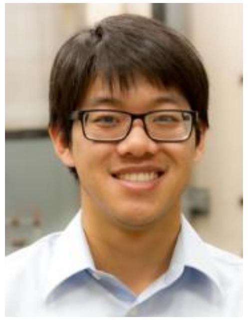

Dr. Gary Li

Dr. Taylor Matlock

Dr. Pablo Guerrero

Ani Thuppul

Mary Konopliv

Angelica Ottaviano

Nolan Uchizono

www.WirzResearchGroup.com
wirz@ucla.com

Fusion and Electric Propulsion (EP) PMI regimes

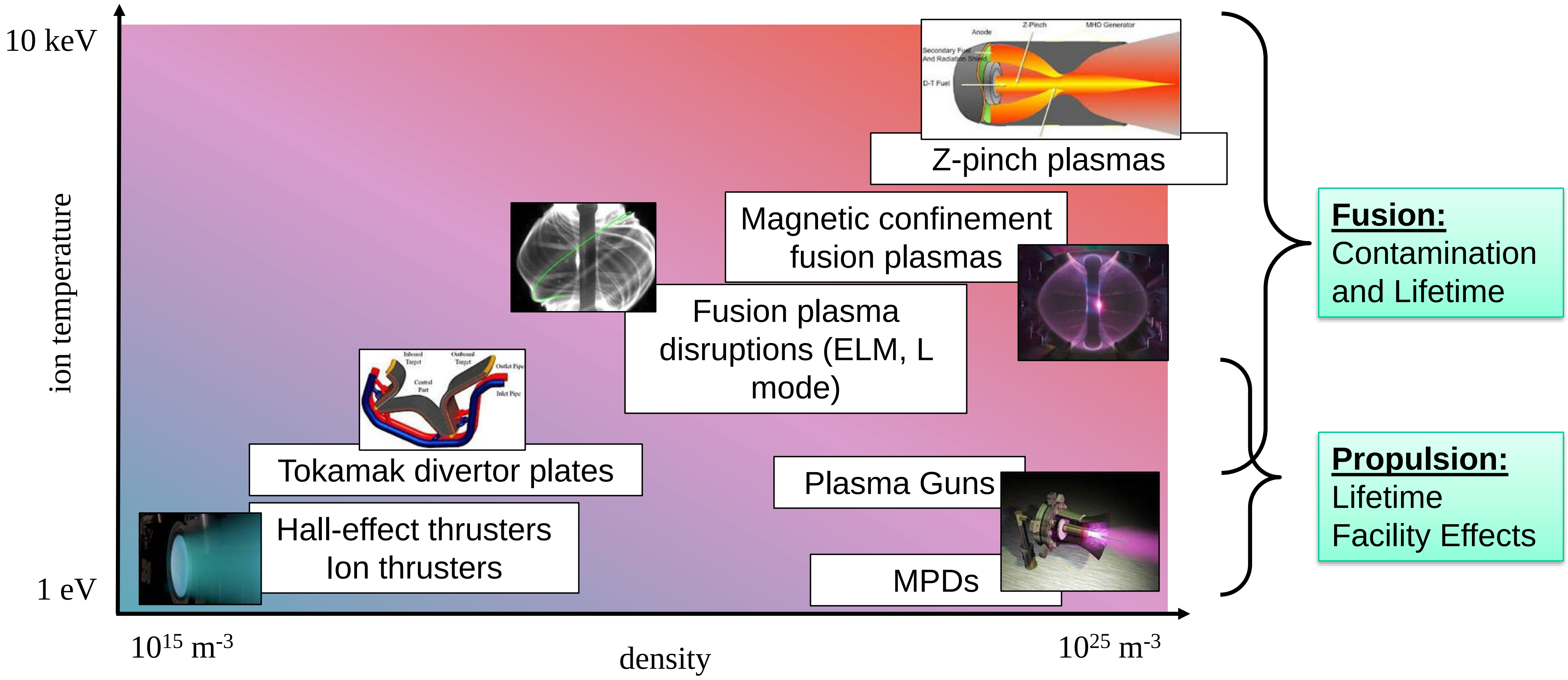

EP and Fusion PMI have complementary and overlapping considerations

Plasma Sputtering Processes

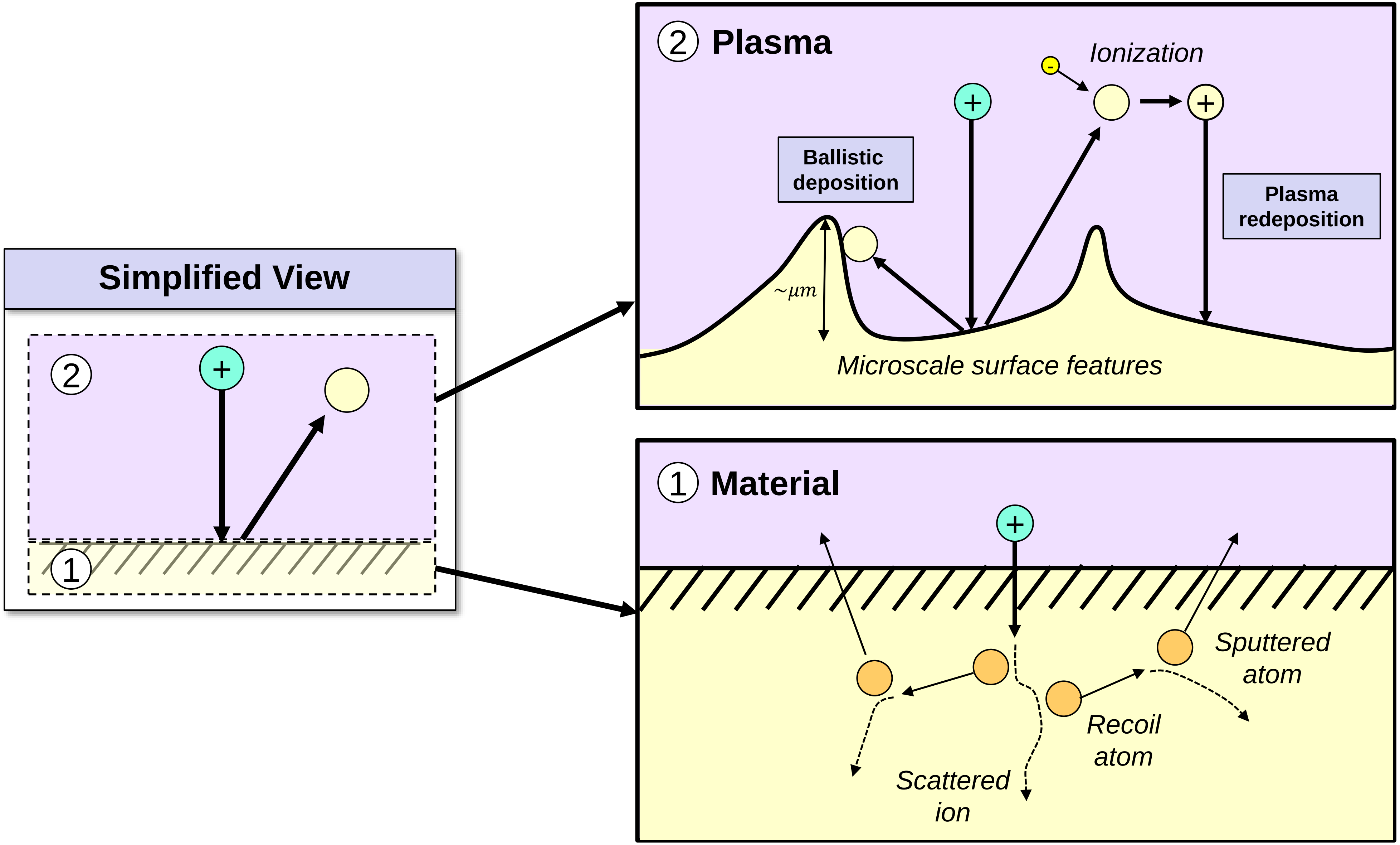

Low Ion Energy Angular Sputtering Profile

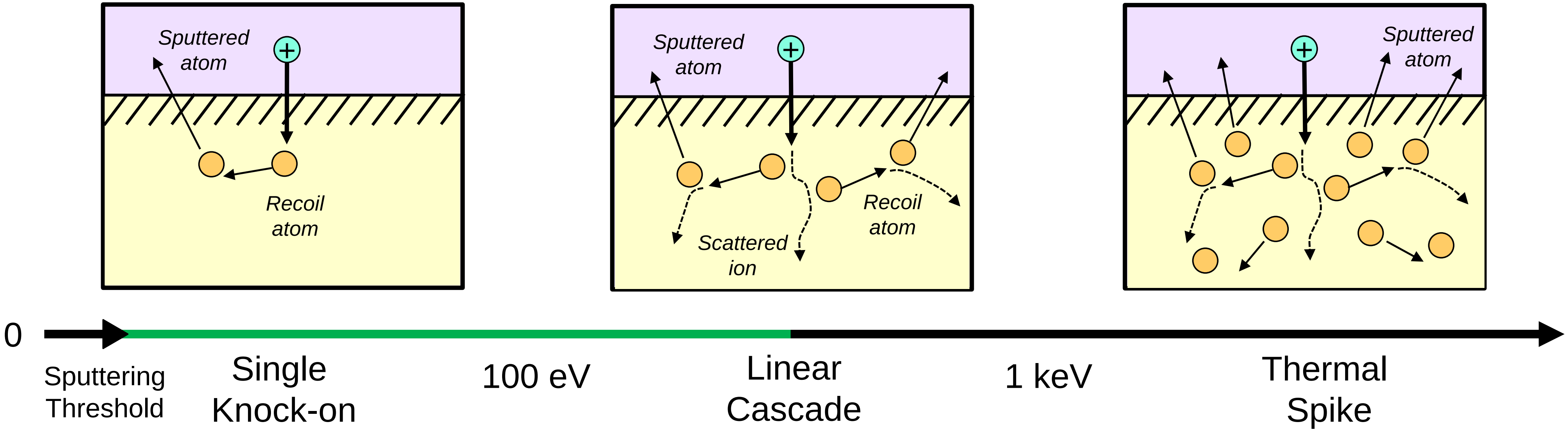

Normal Incidence

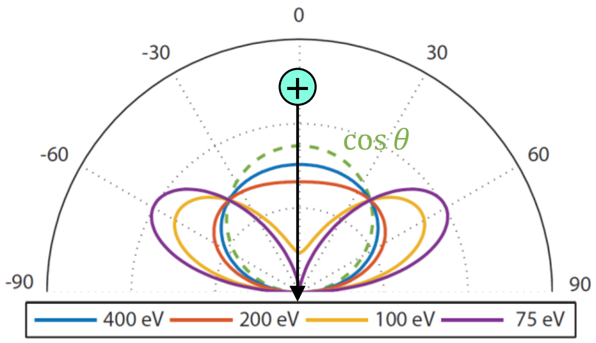

Huerta, Matlock, Wirz (2016) JAP

Angular Sputtering Distribution

$$S(E,\theta,\alpha) \propto \cos\alpha \times \left[1 - \frac{1}{4}\sqrt{\frac{E_{th}}{E}}\left\{\cos\theta\,\gamma(\alpha) + \frac{3}{2}\pi\sin\theta\sin\alpha\cos\phi\right\}\right]$$

$$\gamma(\alpha) = \frac{3\sin^2\alpha - 1}{\sin^2\alpha} + \frac{\cos^2\alpha(\sin^2\alpha + 1)}{2\sin^3\alpha} \times \ln\left(\frac{1+\sin\alpha}{1-\sin\alpha}\right)$$

Normal incidence → “Butterfly” distribution at low energy
Oblique incidence → Forward-biased profile

Yamamura (1982) Rad Eff, Zhang and Zhang (2004) Raf Eff

Oblique Incidence

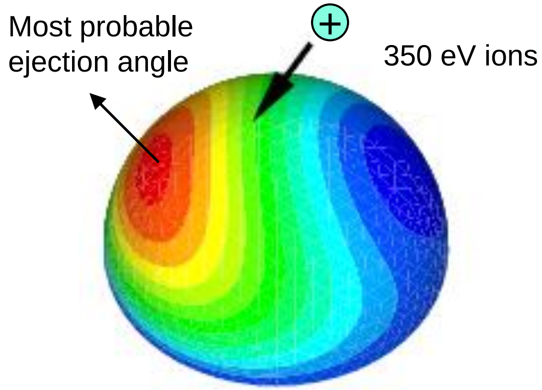

Yalin, A. et al (2007)

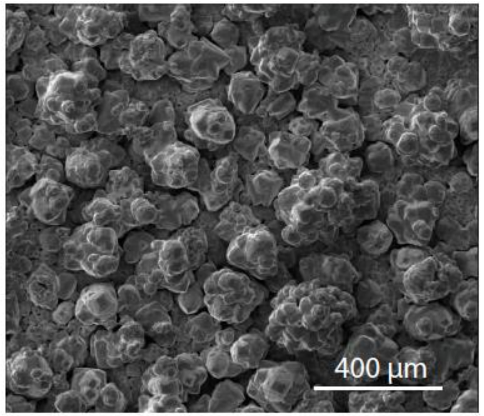

PMI

FOR

COMPLEX SURFACES AND MATERIALS

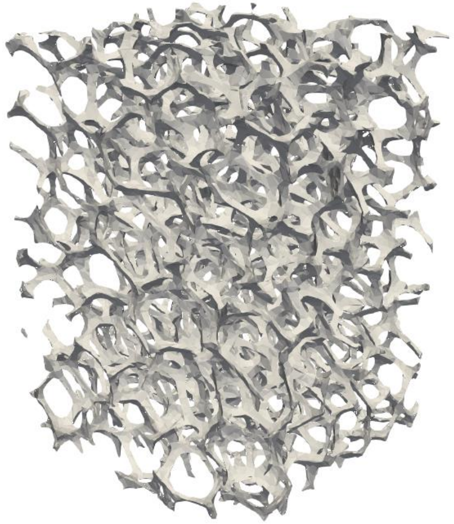

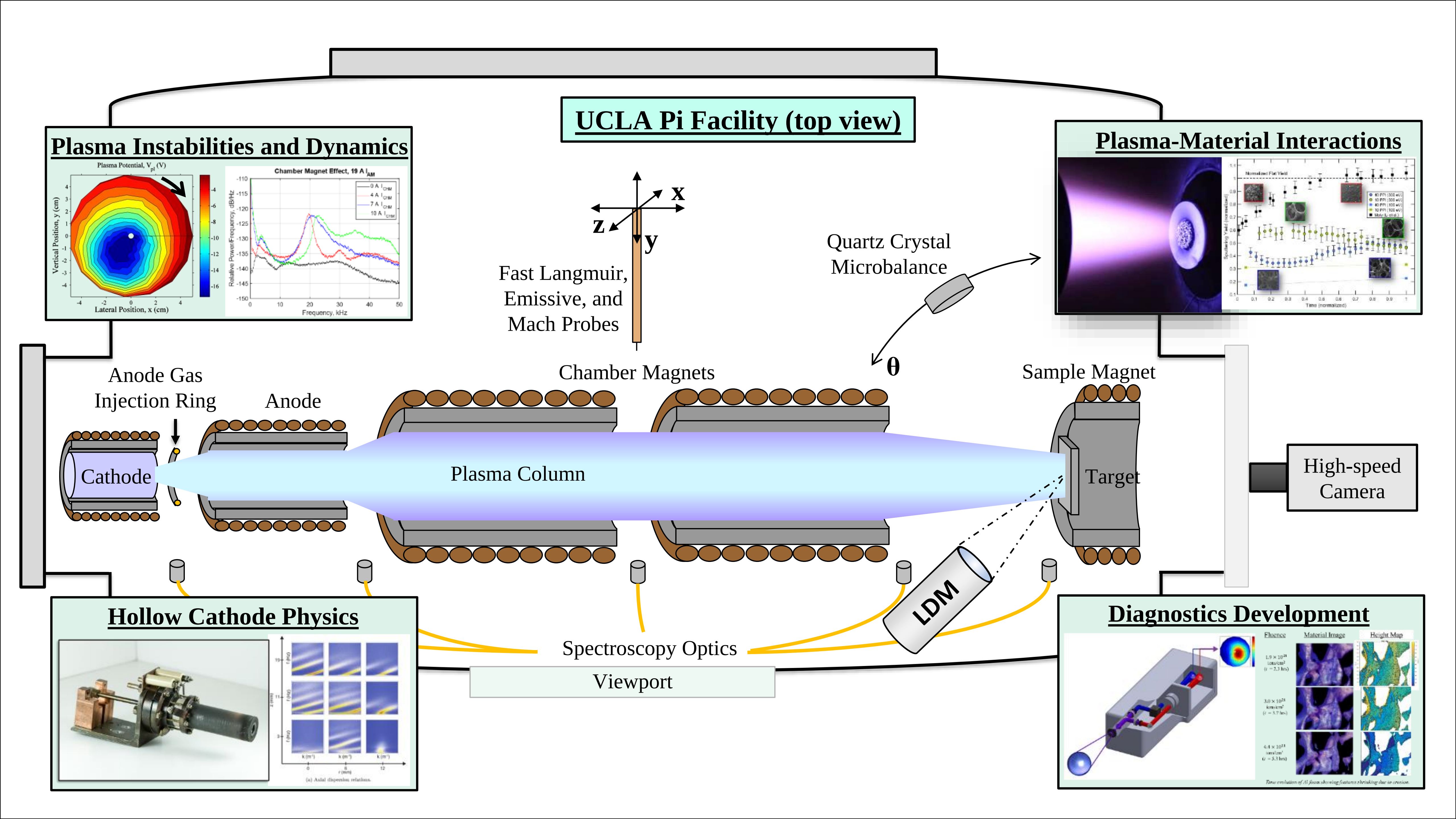

UCLA Pi Facility (top view)
Plasma Instabilities and Dynamics
Plasma-Material Interactions
Hollow Cathode Physics
Diagnostics Development
Fast Langmuir, Emissive, and Mach Probes
Quartz Crystal Microbalance
θ
x
y
z
Anode Gas Injection Ring
Anode
Chamber Magnets
Sample Magnet
Cathode
Plasma Column
Target
High-speed Camera
LDM
Spectroscopy Optics
Viewport
Plasma Potential, V_{pl} (V)
Chamber Magnet Effect, 19 A I_{AM}
Vertical Position, y (cm)
Lateral Position, x (cm)
Relative Power/Frequency, dB/Hz
Frequency, kHz
Fluence
Material Image
Height Map

Plasma-interaction (Pi) Facility at UCLA

Pi is a magnetized, focused hollow cathode plasma onto material target

Type	Diagnostic	Measured Parameters
Non-intrusive	Quartz Crystal Microbalance (QCM)	Differential sputtering rate, sputtering yield
	Long Distance Microscope (LDM)	Surface visualization, height map
	Optical Emission Spectroscopy (OES)	n_e, T_e and n_n of sputterant species
	Laser Induced Fluorescence (LIF)	Ion/neutral velocity distribution function
	Laser Absorption Spectroscopy (LAS)	n_n, T_n of sputterant species
Semi-intrusive	Langmuir Probe	n_e , T_e
	Faraday Probe	1-sided ion flux
	Emissive Probe	Plasma potential
	Retarding Potential Analyzer	Ion energy distribution
Ex-situ	SEM/EDS/TEM/XPS/Laser Profilometry	Comprehensive surface mapping

Parameter	Range
Plasma density	10^{18} m^{-3}
Electron temperature	7 eV
Ion energy	40 to 400 eV
Ion flux to target*	10^{17}cm^{-2}s^{-1}
Target area	≈ 1.8 cm^2

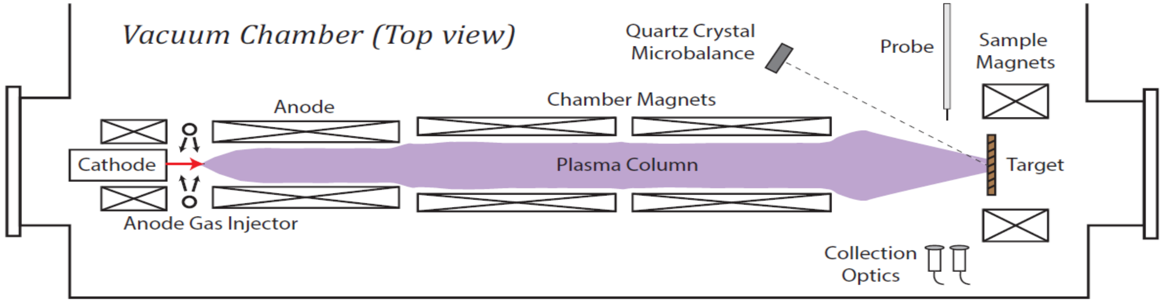

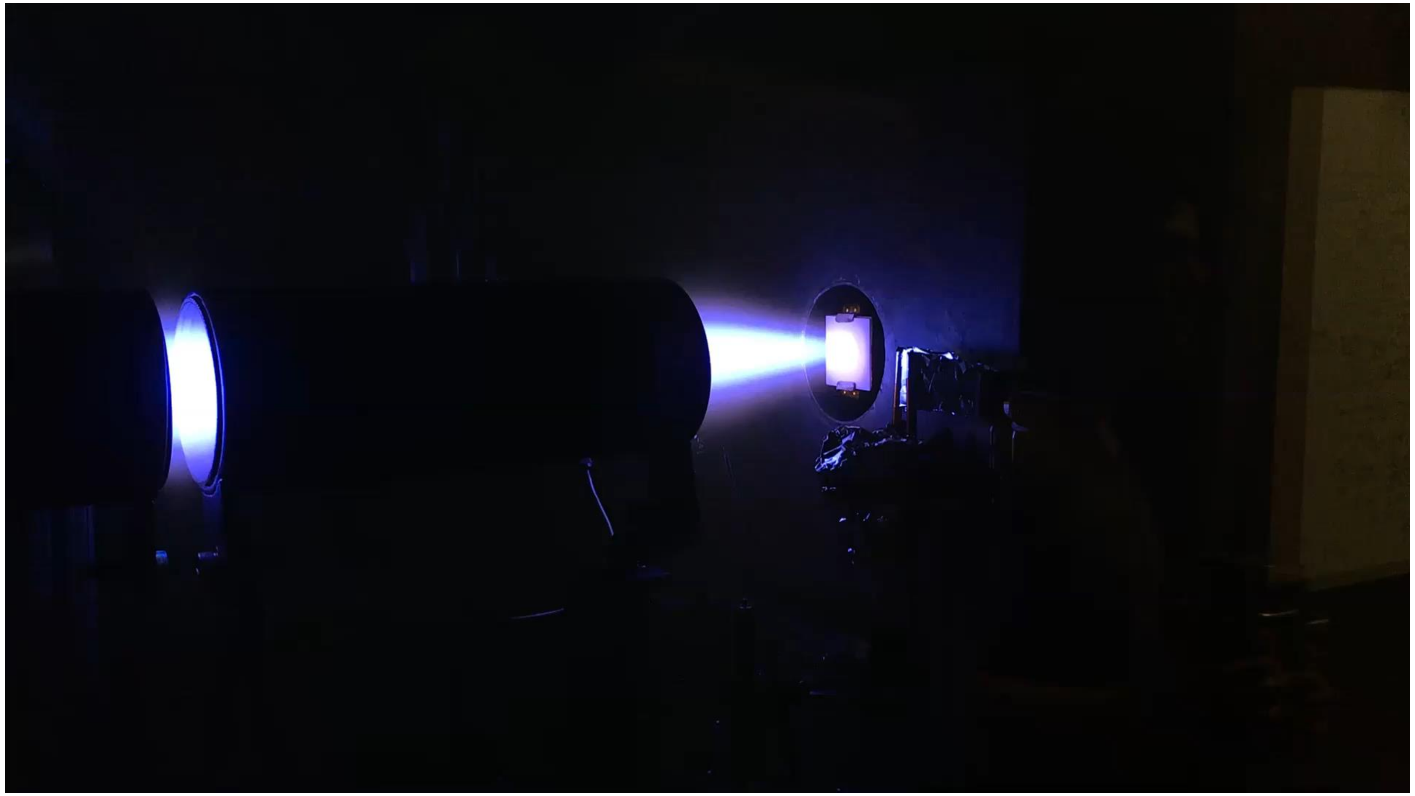

Sputtering Micro-structured Molybdenum

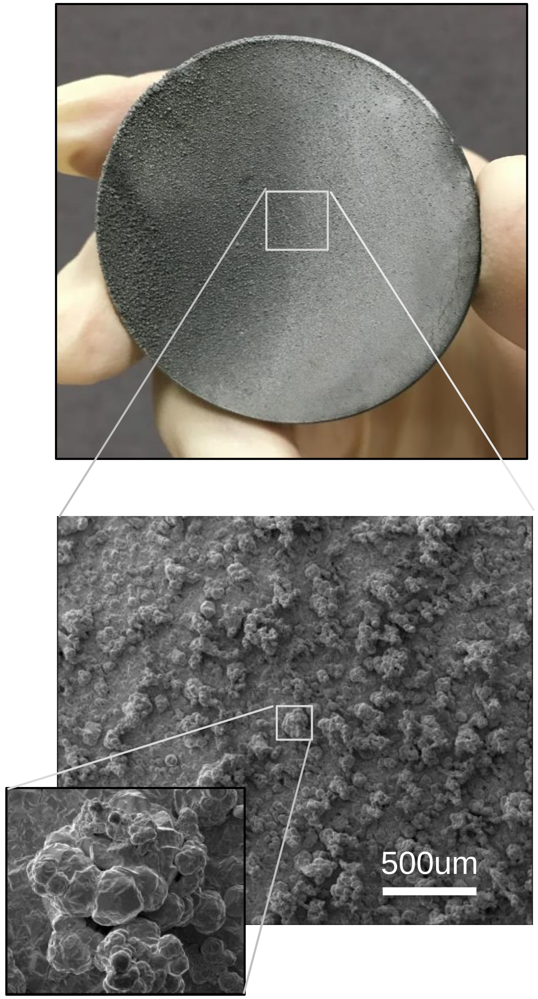

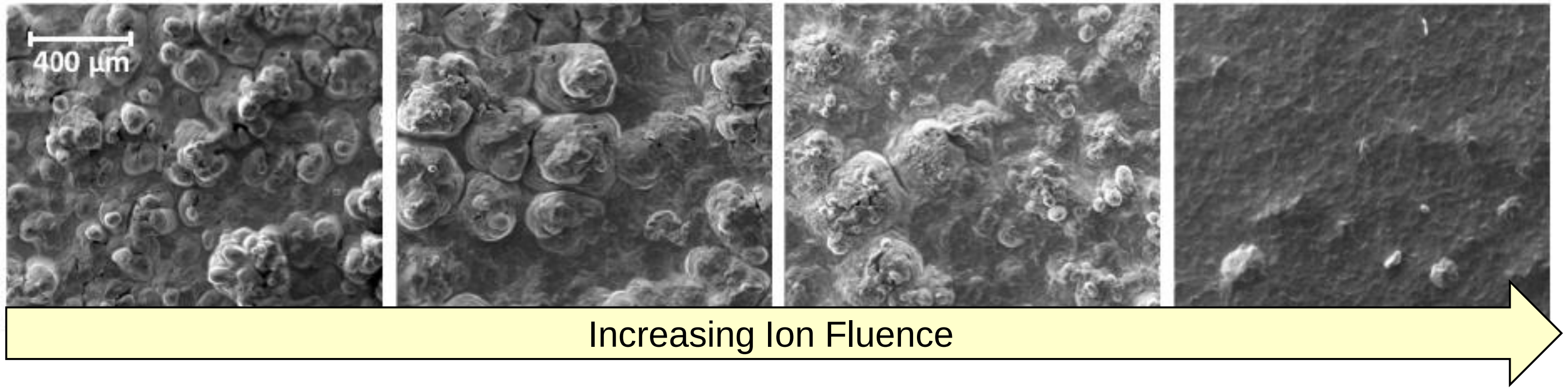

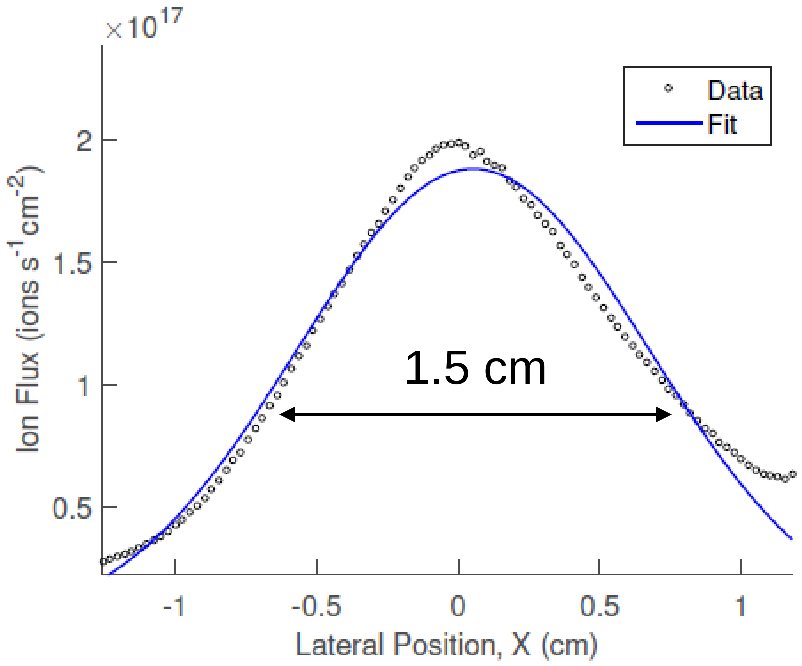

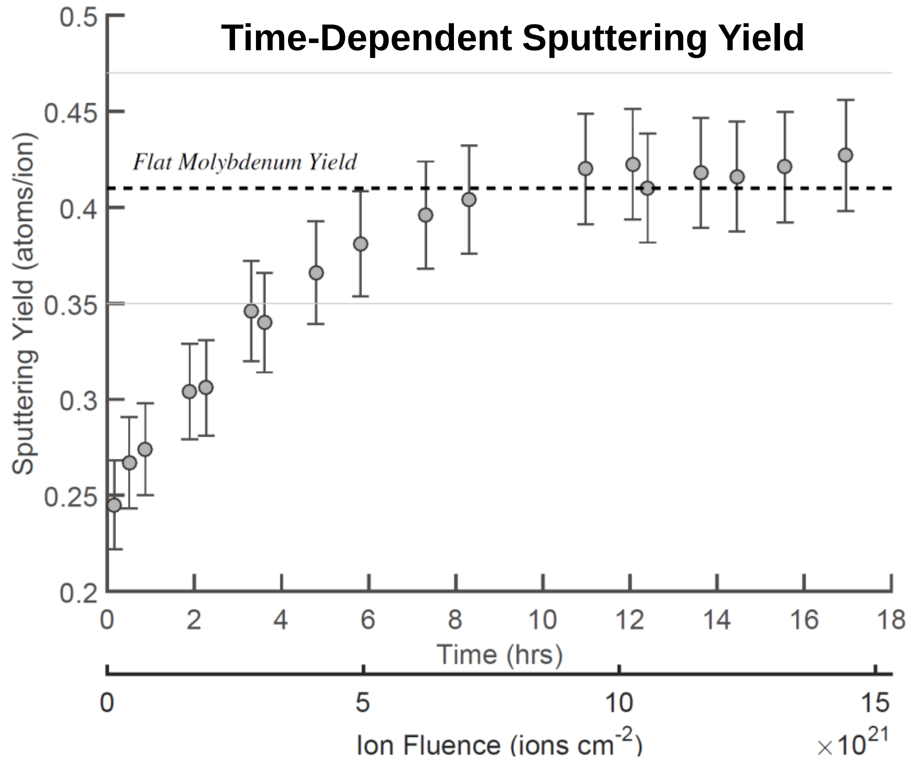

[1] Li, G, Matlock, T, Goebel, D, Dodson, C, Wirz, R, Matthes, C, Ghoniem, N (2017) *Plasma Sources Sci. Tech.*
[2] Matthes, C, Ghoniem, N, Li, G, Matlock, T, Goebel, D, Dodson, C, Wirz, R (2017) *Appl. Surf. Sci.*

Plasma-Resilient Foams?

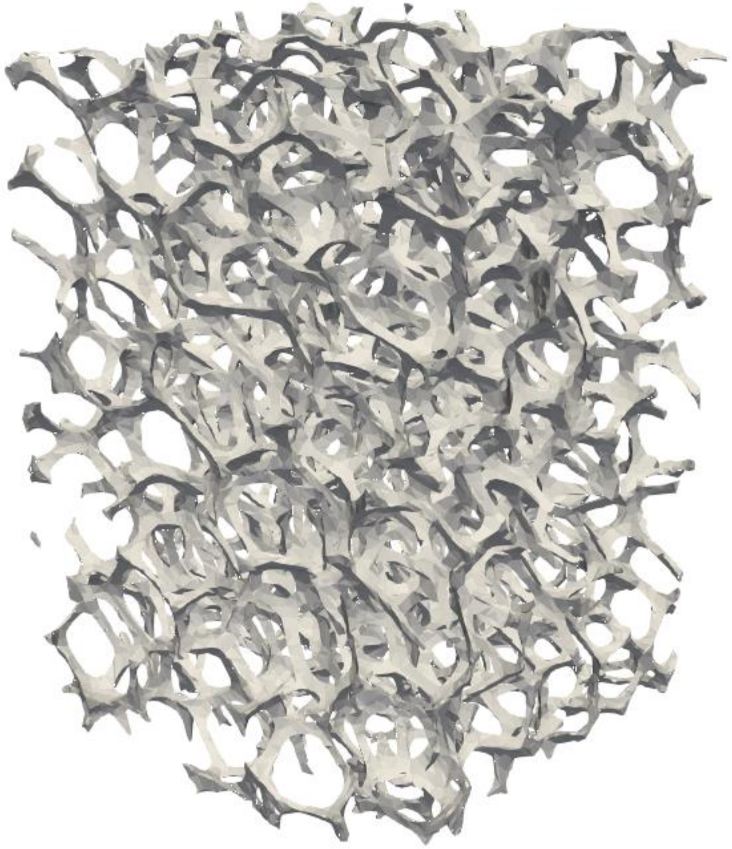

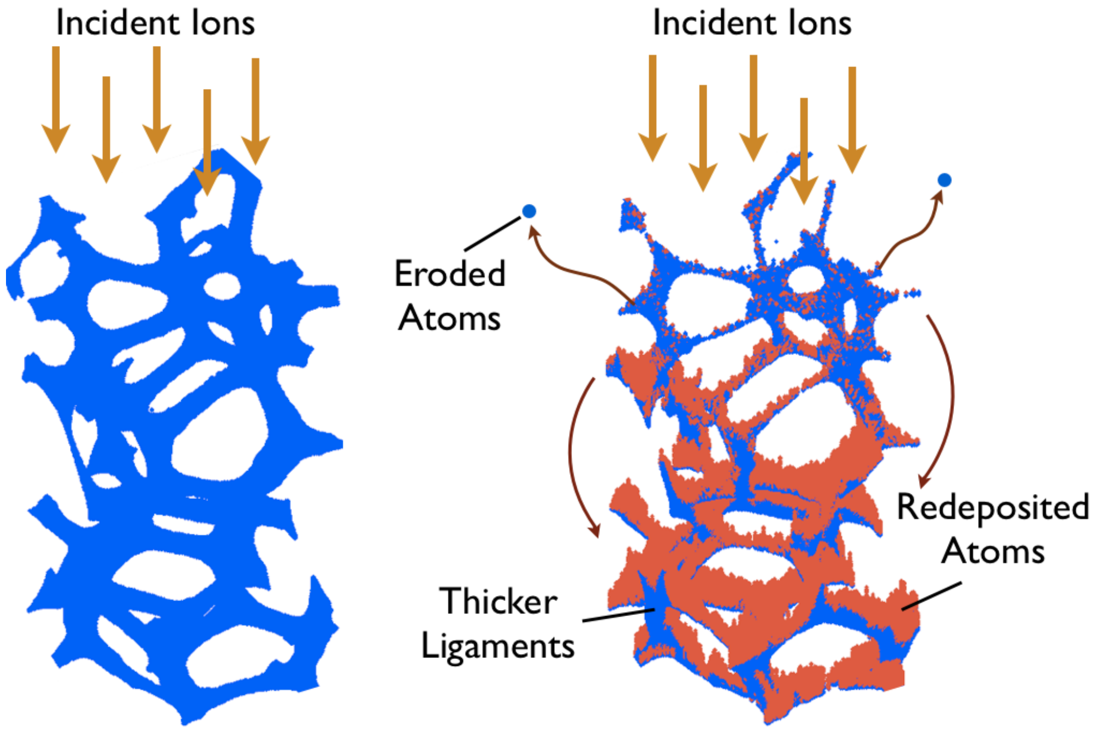

Ghoniem, Marian, Po, Wirz,
“Resilient Self-Healing Materials for the Extreme Environment of Space Electric Propulsion & Power,” AFOSR Aug 2016

Past Research on Foam-like Sputtering

Lunar Regolith as "nanofoam"

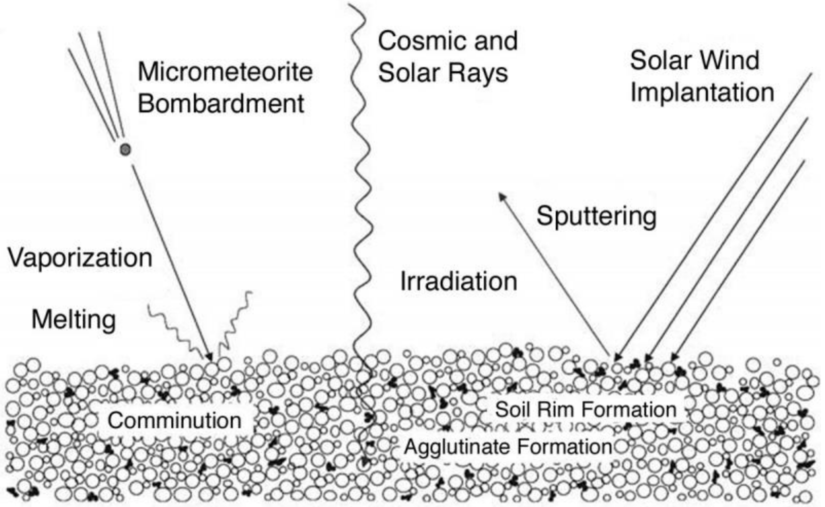

Hapke, B. and Cassidy, W., "Is the moon really as smooth as a billiard ball? Remarks concerning recent models of sputter-fractionation on the lunar surface," Geophysical Research Letters, Vol. 5, No. 4, 1978.

10 keV sputtering of nanofoams

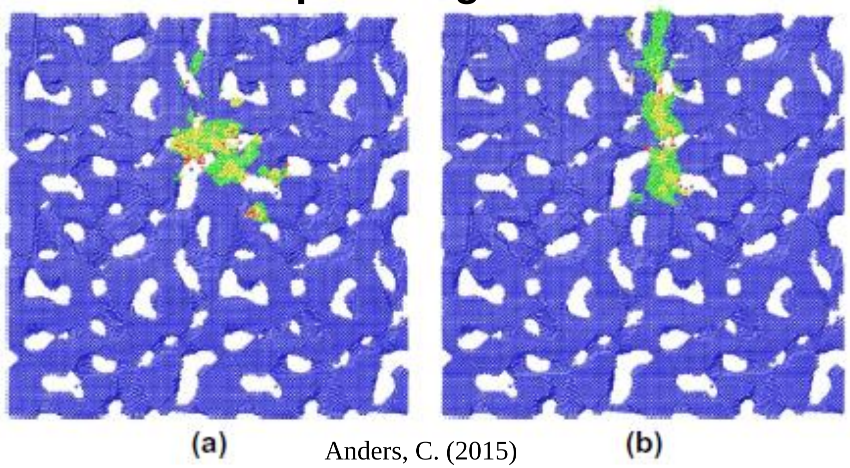

Anders, C. (2015)

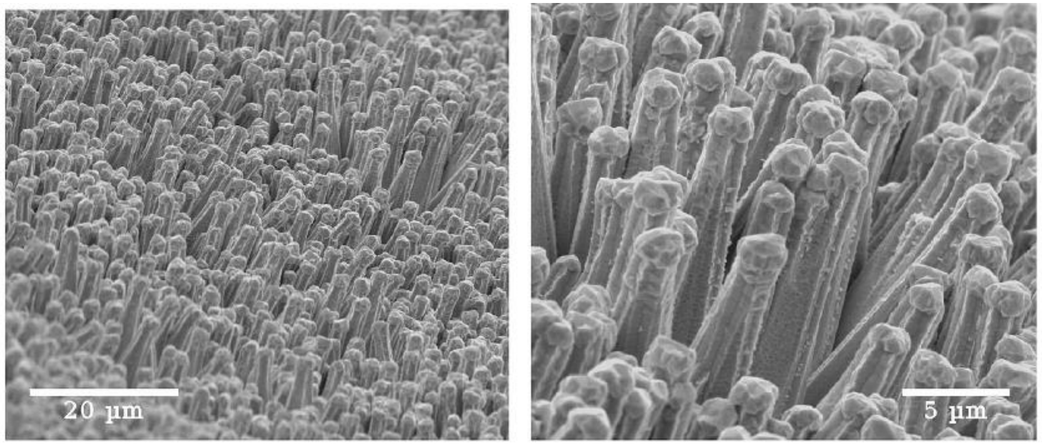

Thermal stress reduction and greater ductility of W-coated Re pillars

Rivera D., Wirz R.E., Ghoniem N.M., "Experimental measurements of surface damage and residual stresses in micro-engineered plasma facing materials," *Journal of Nuclear Materials* 486, pp. 111-121 (April 2017)

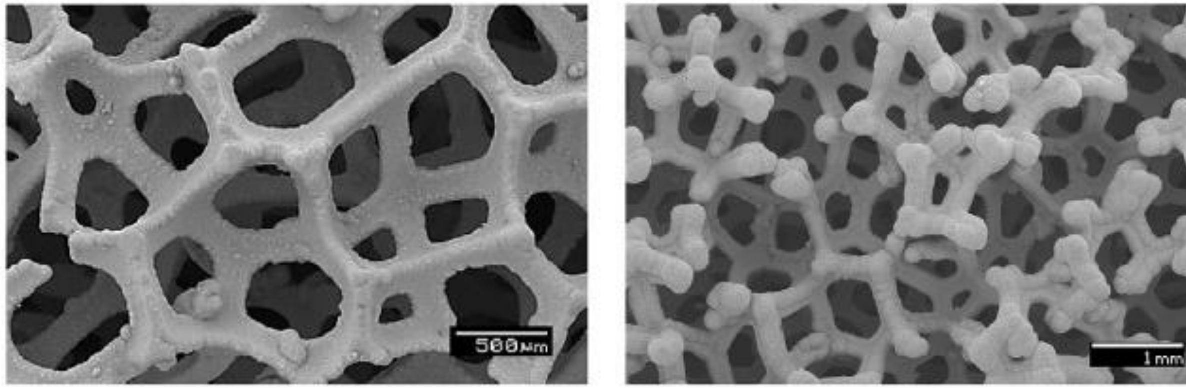

80 – 200 eV Helium Sputtering of Tungsten Foam

Gao, E. et al (2018, 2019)

Long Distance Microscopy and ex-situ diagnostics

In-situ foam erosion visualization

In-situ Long Distance Microscopy for real-time surface evolution video of a foam surface during sputtering erosion

- First-ever in-situ observation of plasma interaction with a textured surface (2016)
- Ottaviano A., Thuppul A., Hayes J., Dodson C., Li G., Chen Z., and Wirz, R.E., “In-situ Microscopy of Ion-Inducted Sputter Erosion of a Featured Surface,” submitted, Rev. Sci. Inst., 2021

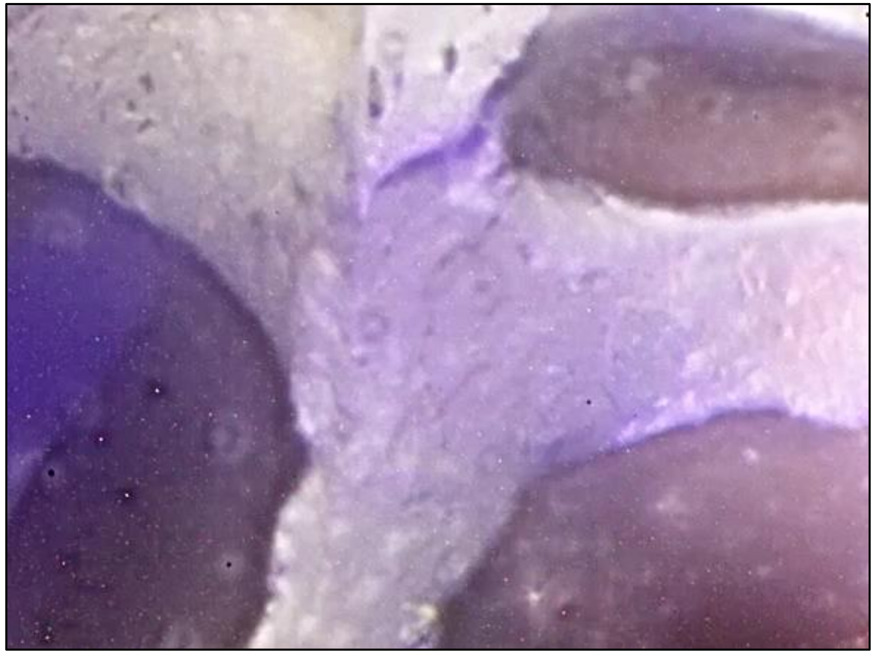

Images

Focus Variation Profilometry

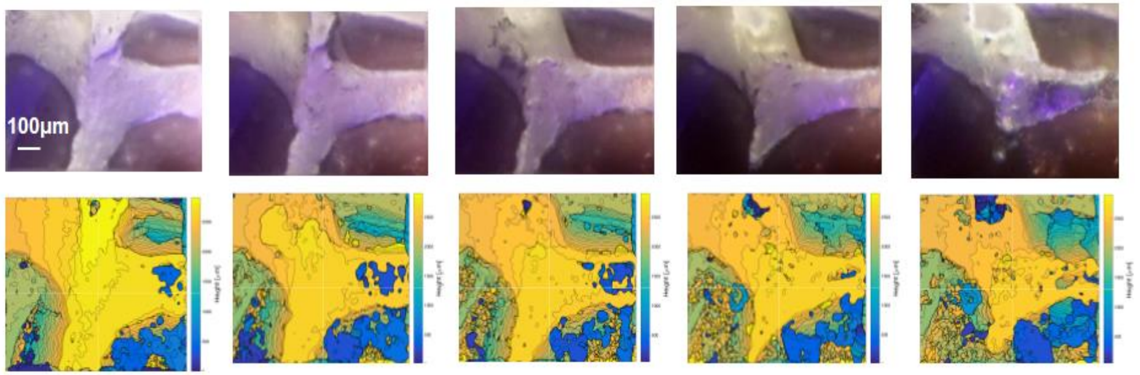

Exposure time:	0 hours	6 hours	12 hours	18 hours	24 hours
Fluence:	$0\ ions/cm^2$	$2.16 \times 10^{21} ions/cm^2$	$4.32 \times 10^{21} ions/cm^2$	$6.48 \times 10^{21} ions/cm^2$	$8.64 \times 10^{21} ions/cm^2$

Pre-plasma exposure

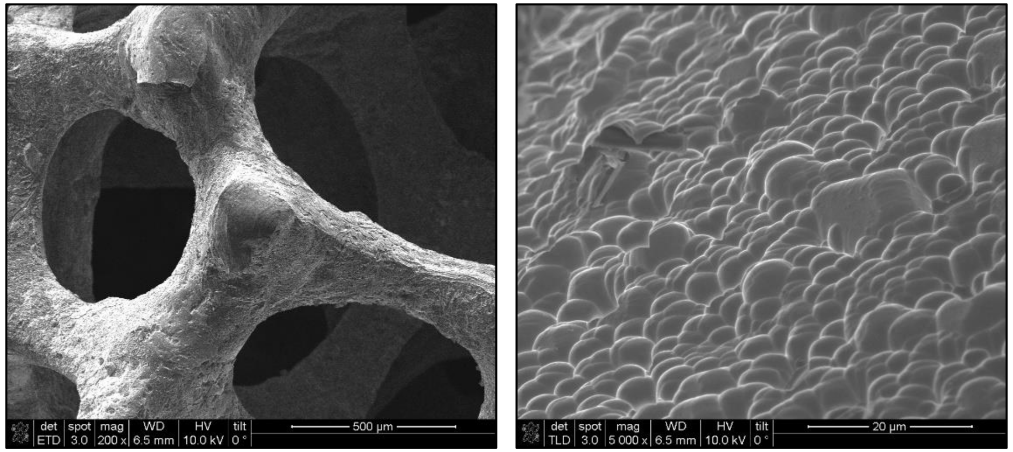

Post-plasma exposure

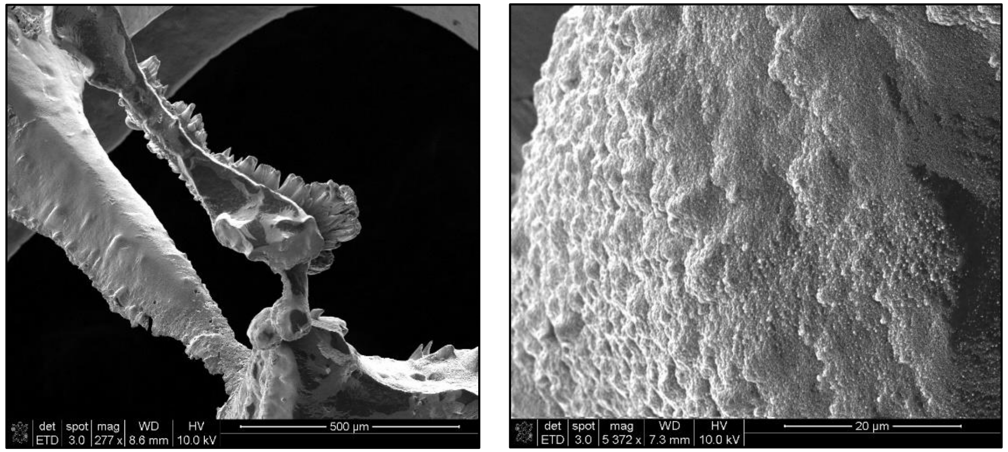

Persistent Sputtering Reduction & Plasma-Infused Materials

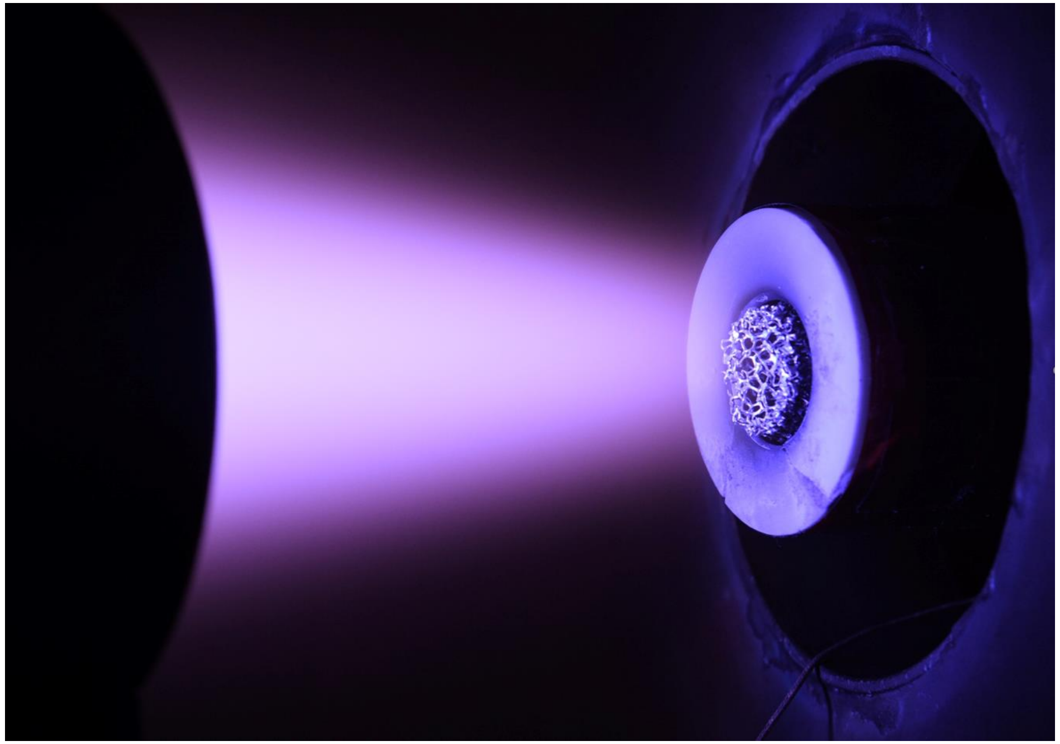

Li G., Wirz R.E., "Persistent Sputtering Yield Reduction in Plasma-Infused Foams," *Physical Review Letters*, 126 (3), 035001 (2021) https://doi.org/10.1103/PhysRevLett.126.035001

Plasma Sheaths and Foams

1D Ion Sheath ($\Delta\phi_s \gg T_e$)

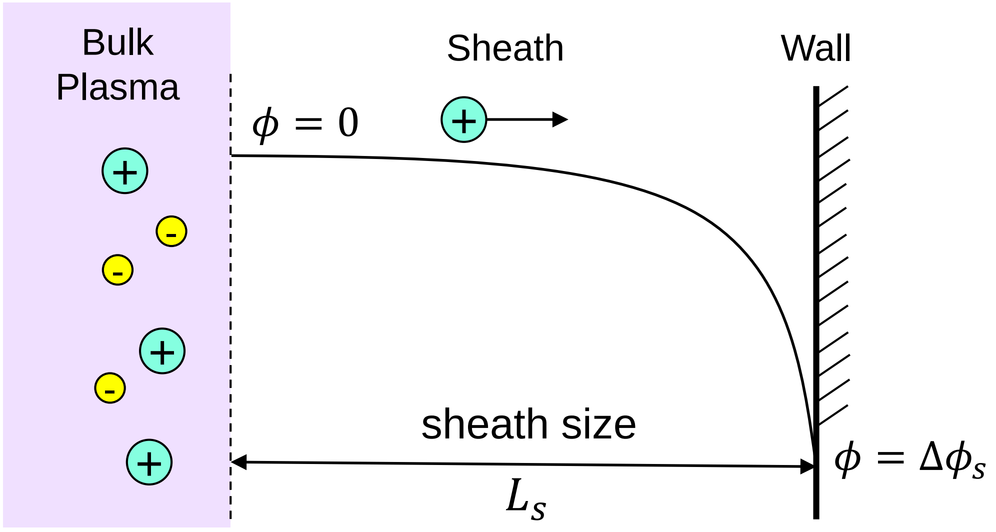

Ions accelerated through sheath $E_{ion} = \Delta\phi_s$

2D Ion Sheath and Foam Surface

Small Pores $D \ll L_s$ | Large Pores $D \gg L_s$

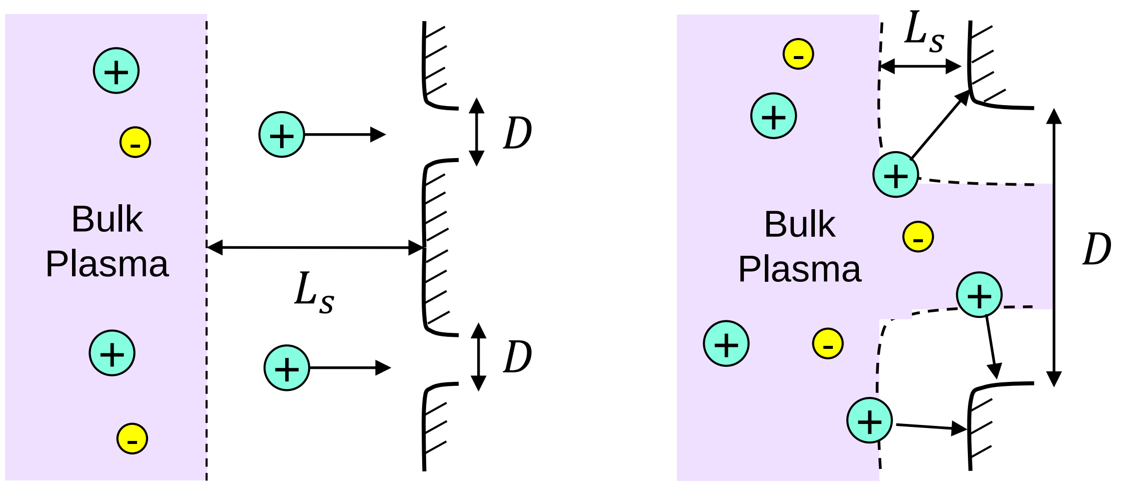

Sheath forms outside foam. | Sheath conforms to surface.

Child-Langmuir Sheath $\quad \frac{L_s}{\lambda_D} = \frac{\sqrt{2}}{3}\left(\frac{2e\Delta\phi_s}{T_e}\right)^{3/4}$

Debye Length $\quad \lambda_D^2 = \frac{\epsilon_0 k_B T_e}{n_e e^2}$

Plasma Infusion Parameter, $\boldsymbol{\xi = \frac{D}{L_s}}$

$$\xi = \frac{D}{L_s} \propto \frac{D\sqrt{n_e}\,T_e^{1/4}}{\Delta\phi^{3/4}}$$

$\xi \ll 1$ ➔ Plasma-Facing
$\xi \gg 1$ ➔ Plasma-Infused
$\xi \approx 1$ ➔ Transition Region

[1] Baalrud, S. et al (2020) Plasma Sources Sci. Tech.

Aluminum Foam Experiments

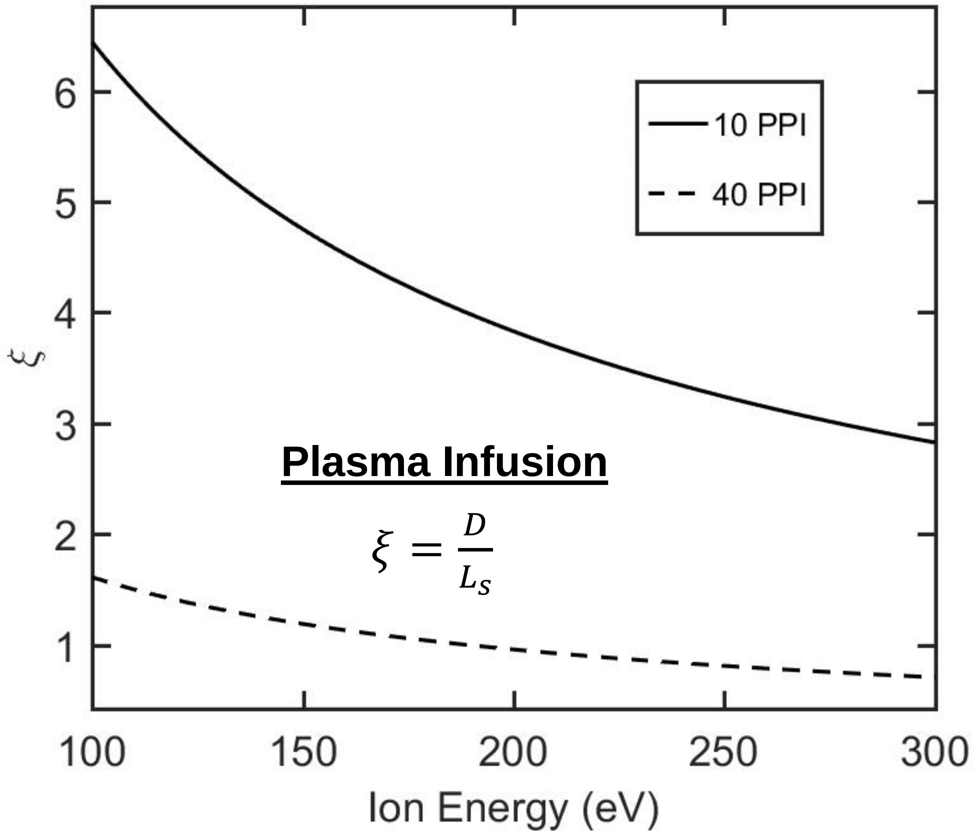

40 PPI

$\xi_{40} \approx 0.7 - 1.7$

Transitional Regime

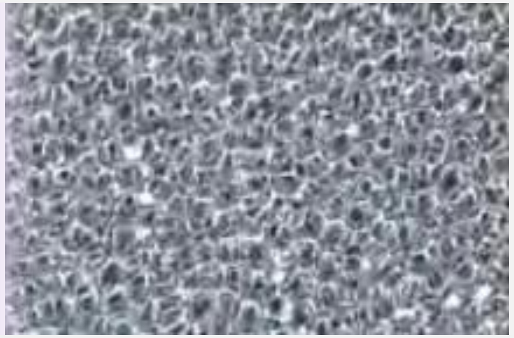

10 PPI

$\xi_{10} = 2.8 - 6.5$

Partially Plasma-infused

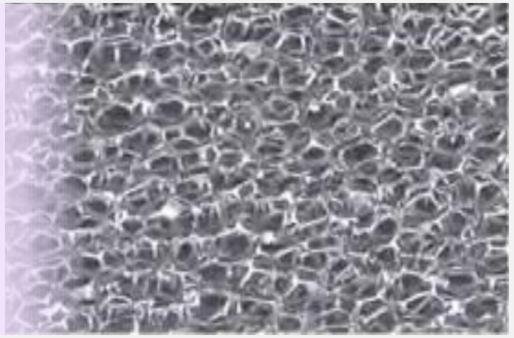

Test Conditions

- 100 - 300 eV argon ions
- 2×10^{-6} Torr (base)
- 30 hrs total duration over 3 days

*PPI = Pores Per Inch

Sheath size in Pi

$$\lambda_D = \sqrt{\frac{\epsilon_0 k_B T_e}{n_e e^2}} \sim 50\mu m \qquad n_e \sim 10^{17}, \quad T_e \sim 5\ eV, \quad \Delta\phi_s \sim 300\ V$$

$$L_s = \frac{\sqrt{2}}{3}\left(\frac{2e\Delta\phi_s}{T_e}\right)^{3/4}\lambda_D = 850\ \mu m$$

Foam Geometry

10 PPI → D = 1.52 mm
40 PPI → D = 381 μm

UCLA PLASMA & SPACE PROPULSION

Test Observations – 40 PPI Al foam

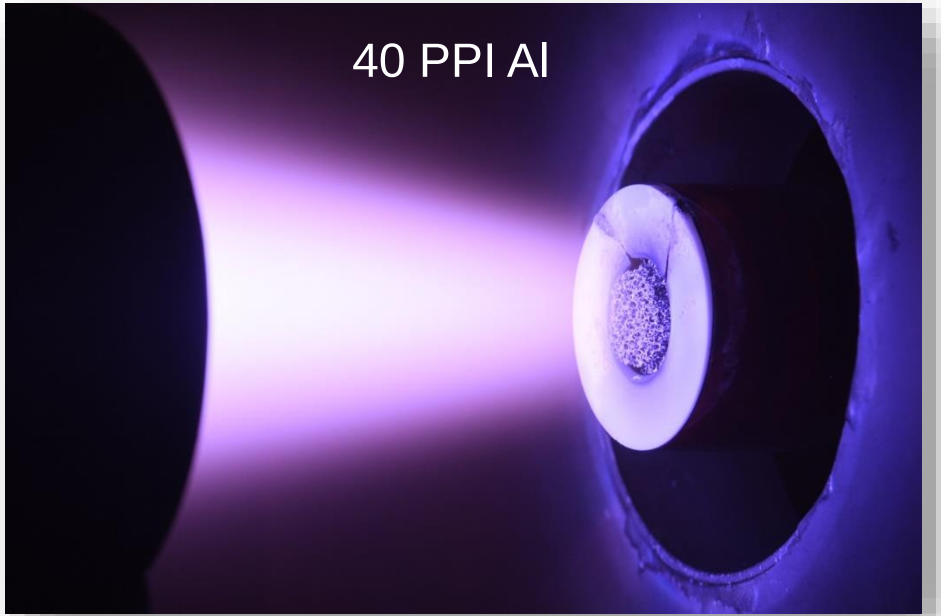

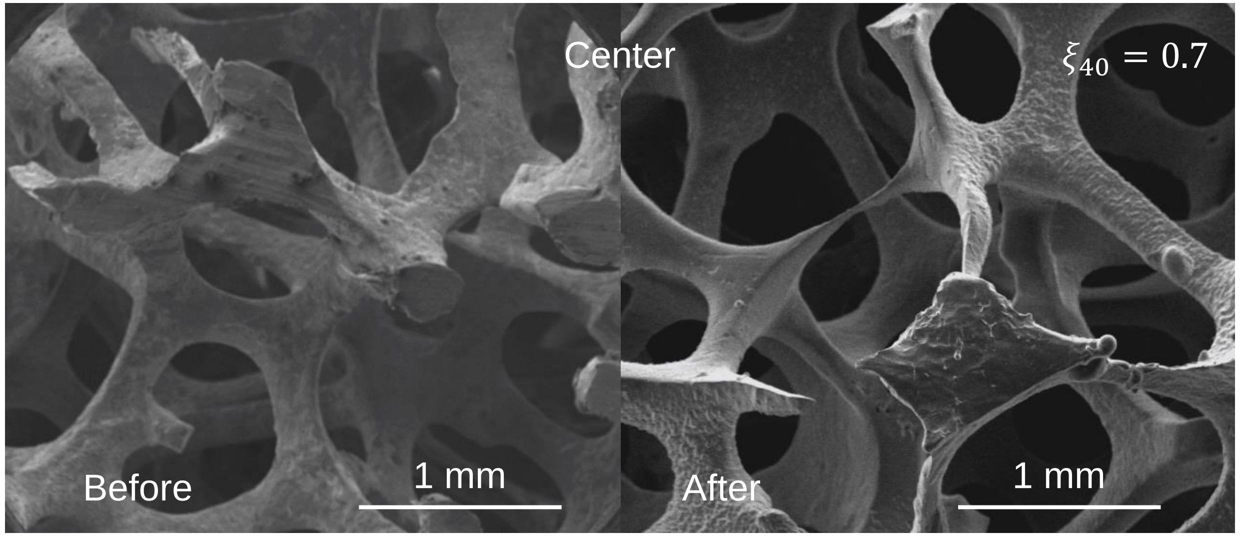

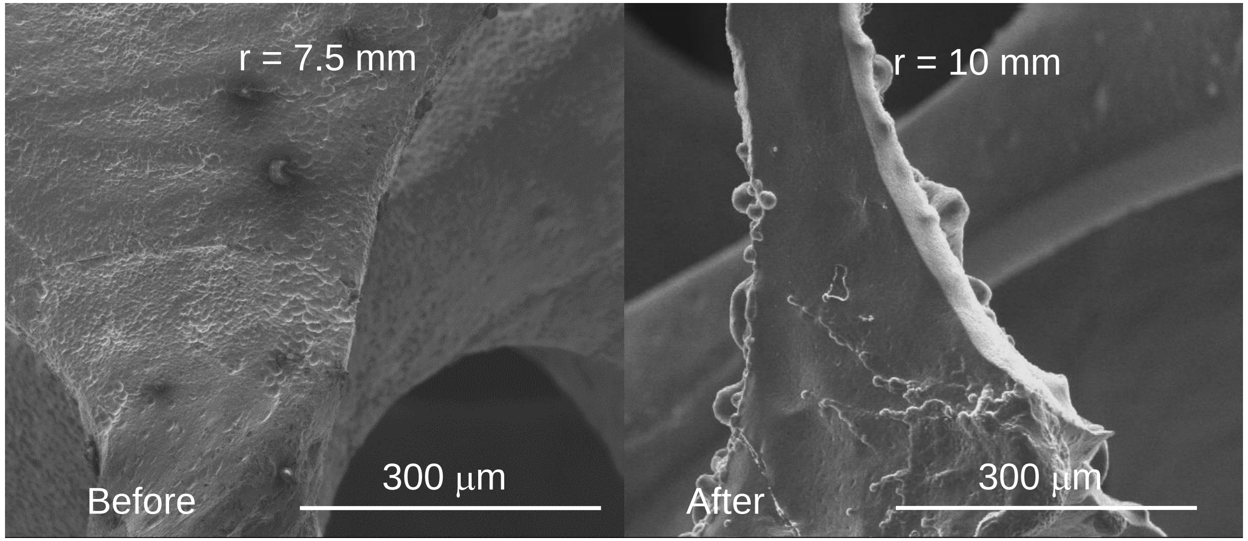

Note: different features

Test Observations – 10 PPI Al foam

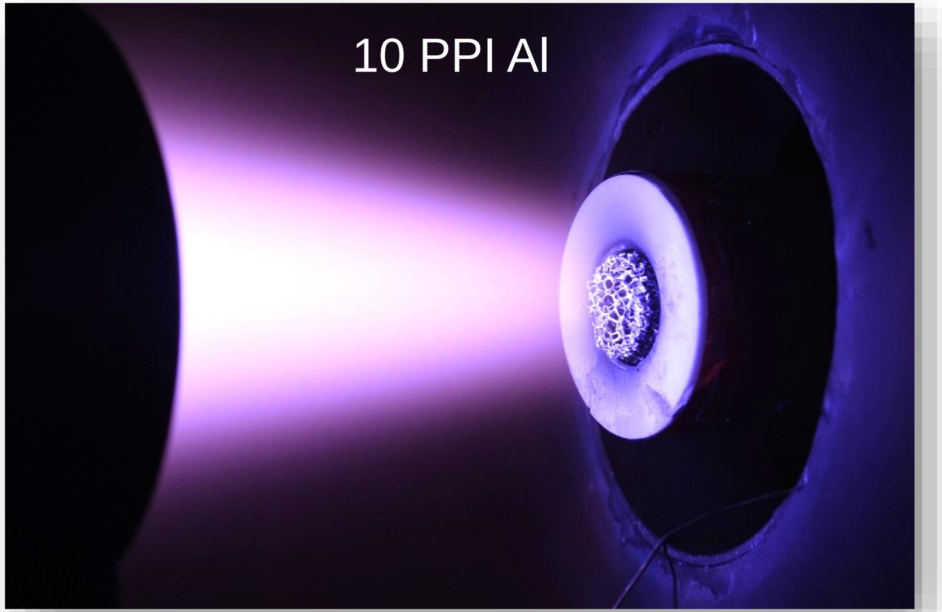

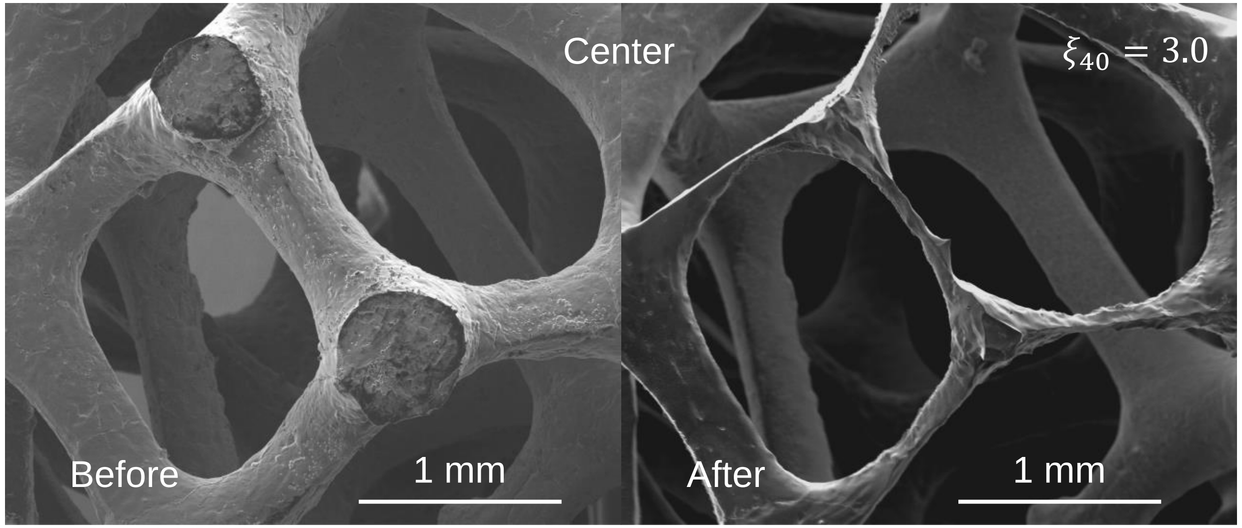

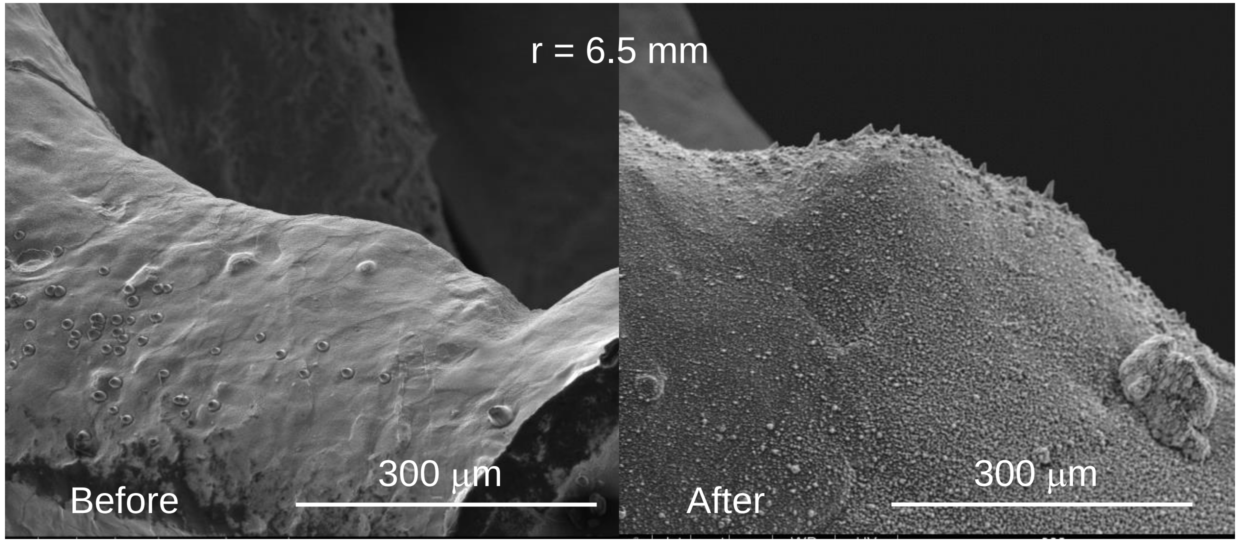

Sputtering Yield of Volumetrically Architectured Materials

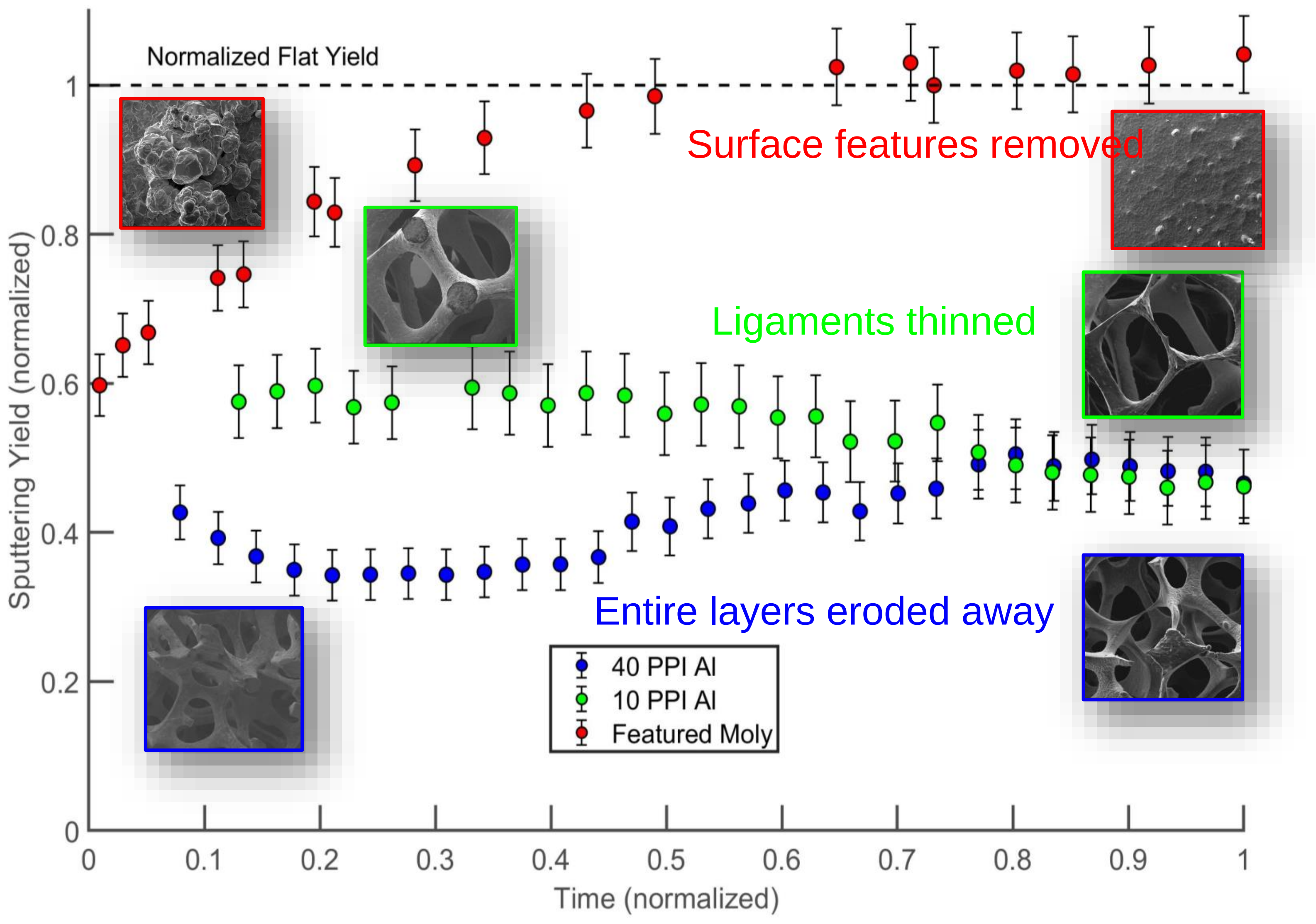

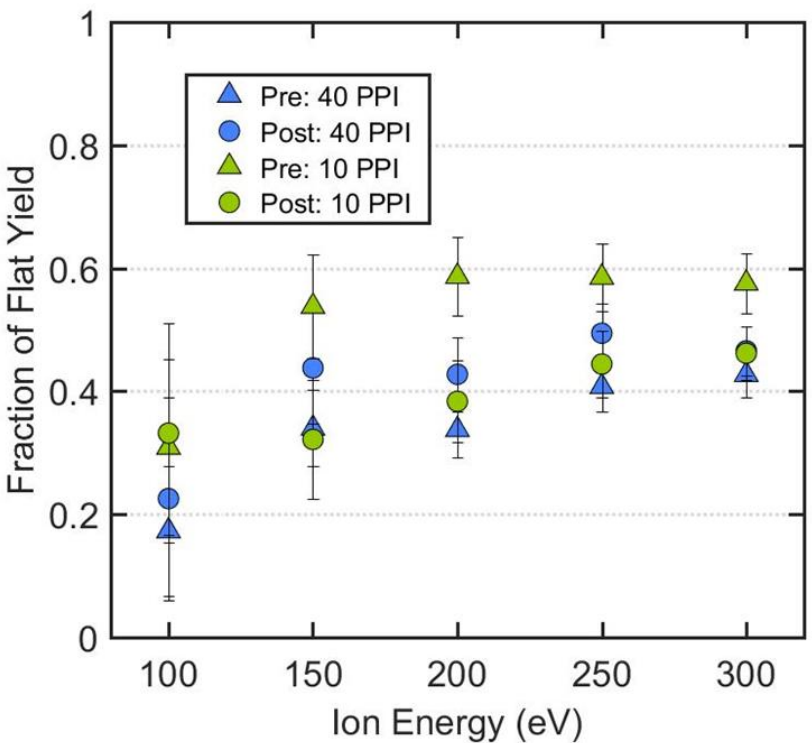

Analysis of Plasma-foam Sputtering Behavior

3D cage geometry

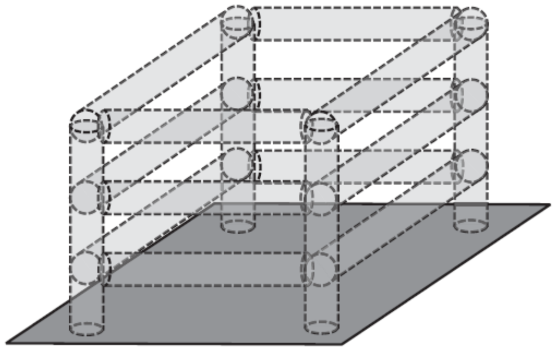

Huerta, Patino, Wirz (2018) J. Phys. D

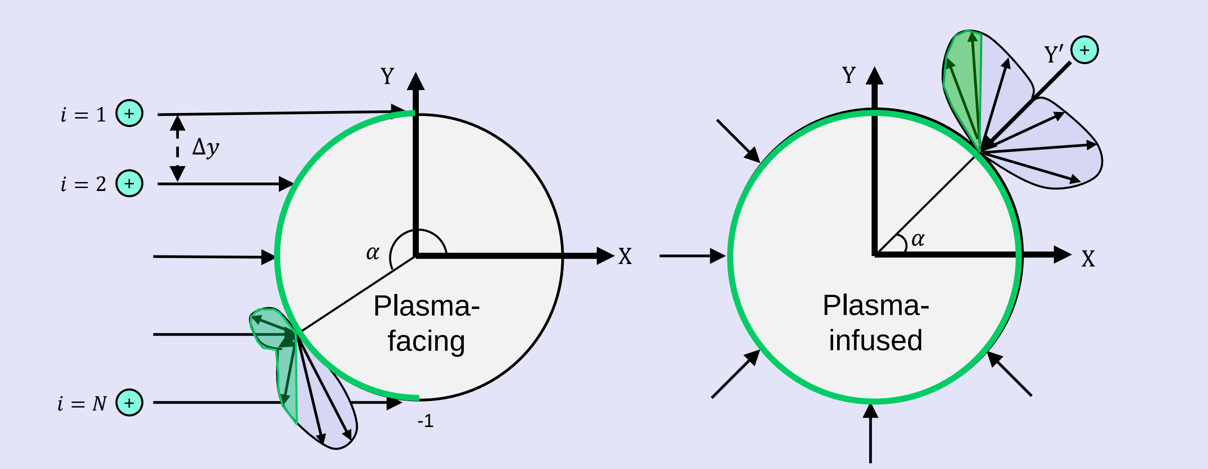

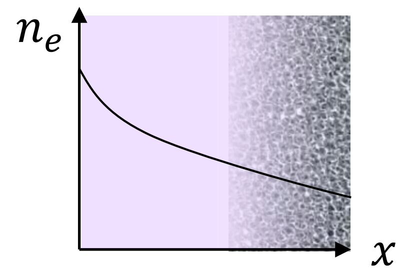

$f_{\nabla n}^{(n)}$: density gradient term

*for plasma infused cases only

$$Y_{eff} = Y_{flat} \sum_{n=1}^{N} \left(1 - p^{(n)}\right) f_A f_\beta \left(1 - f_{dep}^{(n)}\right) f_{\nabla n}^{(n)}$$

Opacity

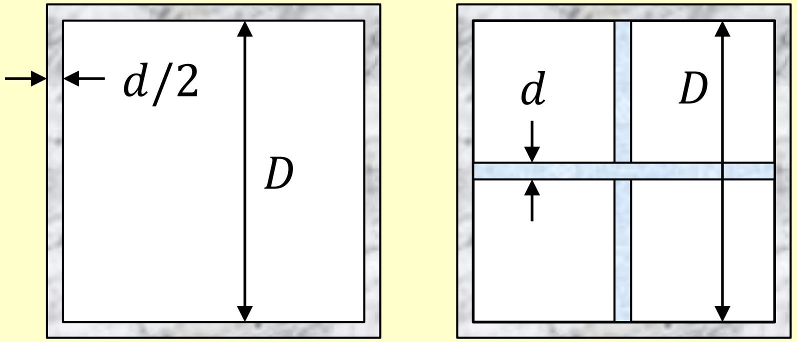

1st layer 2nd layer

Ballistic Deposition

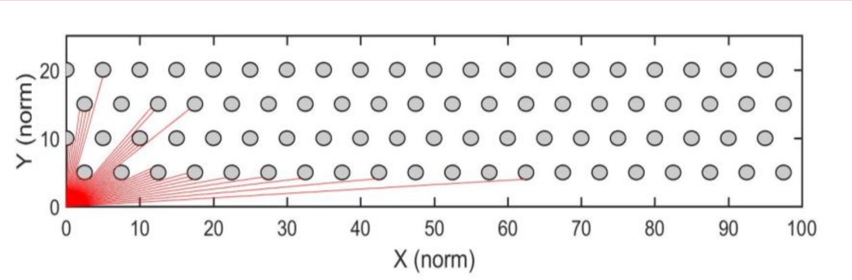

Area Factor, f_A, and Backsputter Fraction, f_β

Plasma-facing

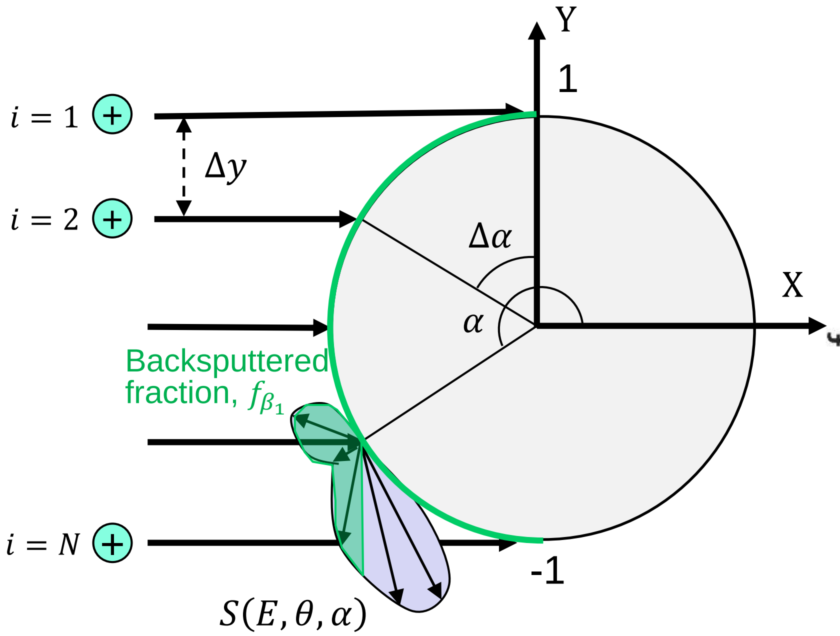

$$f_\beta = \frac{1}{N}\sum f_{\beta_i} \sim 0.8$$

Numerically iterate through ion impacts.

$$f_A = \frac{dD}{dD} = 1$$

Dependent on ion energy

Sensitive to sputtering threshold energy.

Low Energy Angular Sputtering Profile

$$S(E,\theta,\alpha) \propto \cos\alpha \times \Big[1 - \frac{1}{4}\sqrt{\frac{E_{th}}{E}}\Big\{\cos\theta\,\gamma(\alpha) +$$

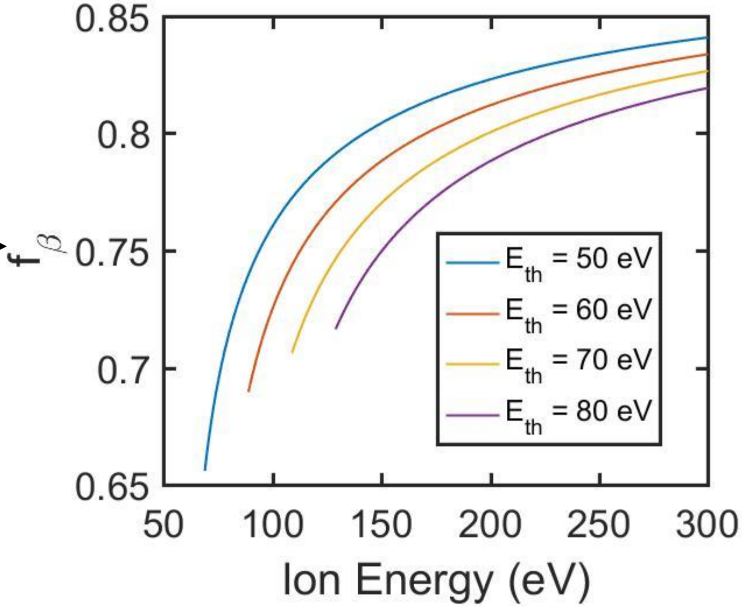

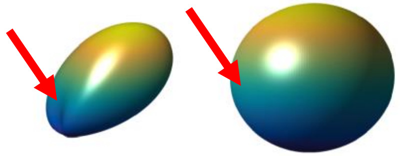

Plasma-infused

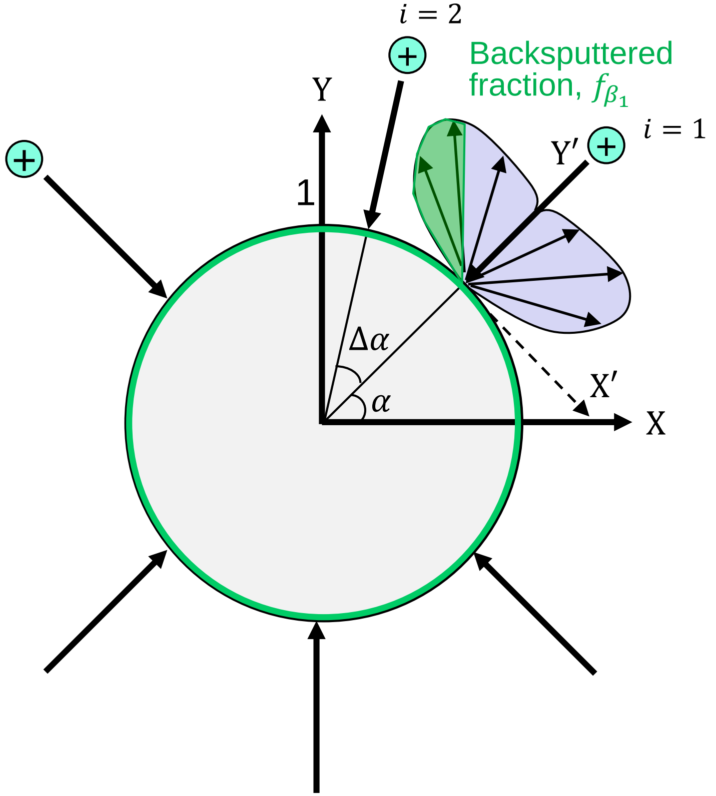

$$f_\beta = \frac{1}{N}\sum f_{\beta_i} = 0.5$$

Symmetry

$$f_A = \frac{2\pi(d/2)D}{dD} = \pi$$

Ballistic Deposition Factor, f_{dep}

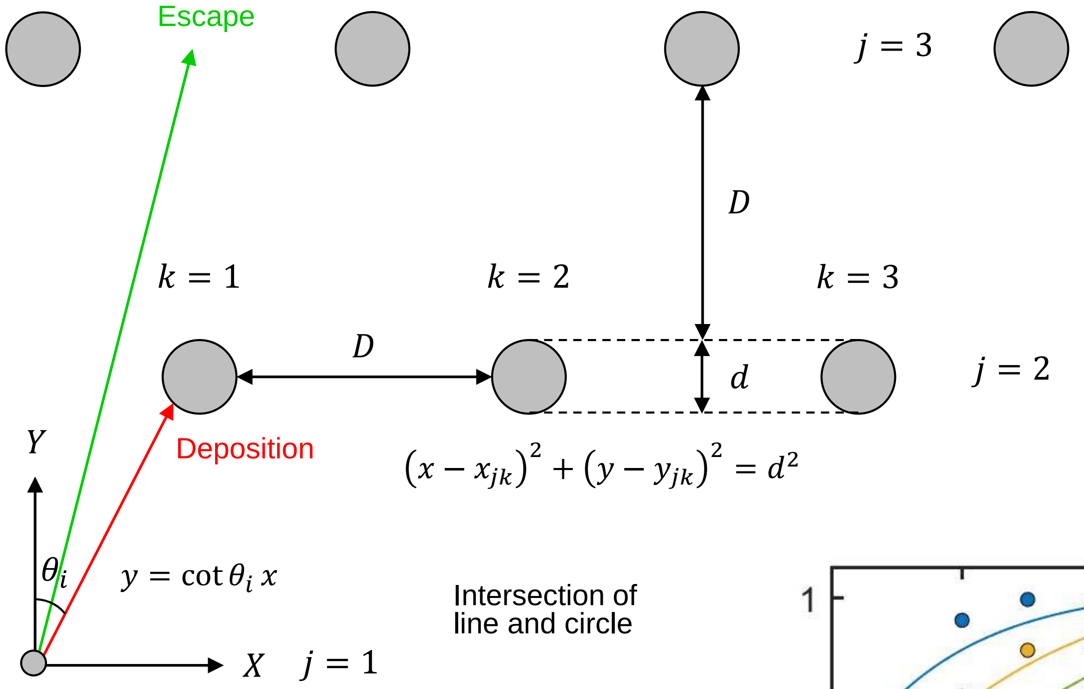

Point source sputterant emission

$$f_{dep} = f_0 + \left[1 - \exp\left(-\frac{N}{N'}\right)\right]$$

Analogous to particle mean free path scenario.

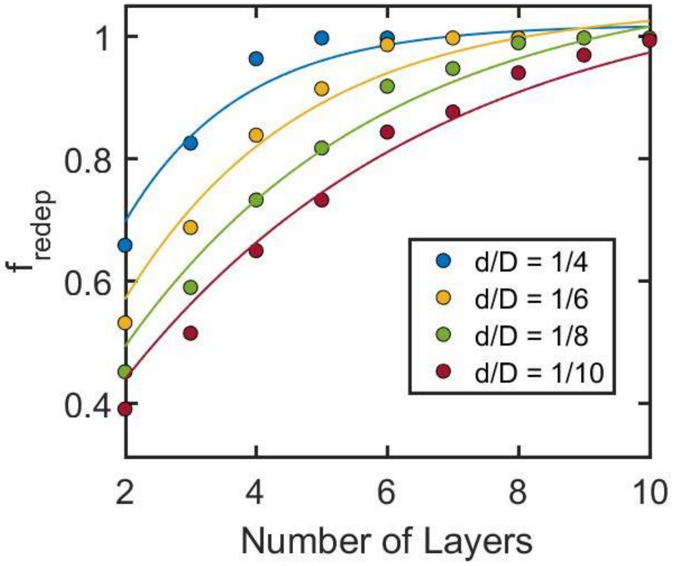

Example of Varying Ratios

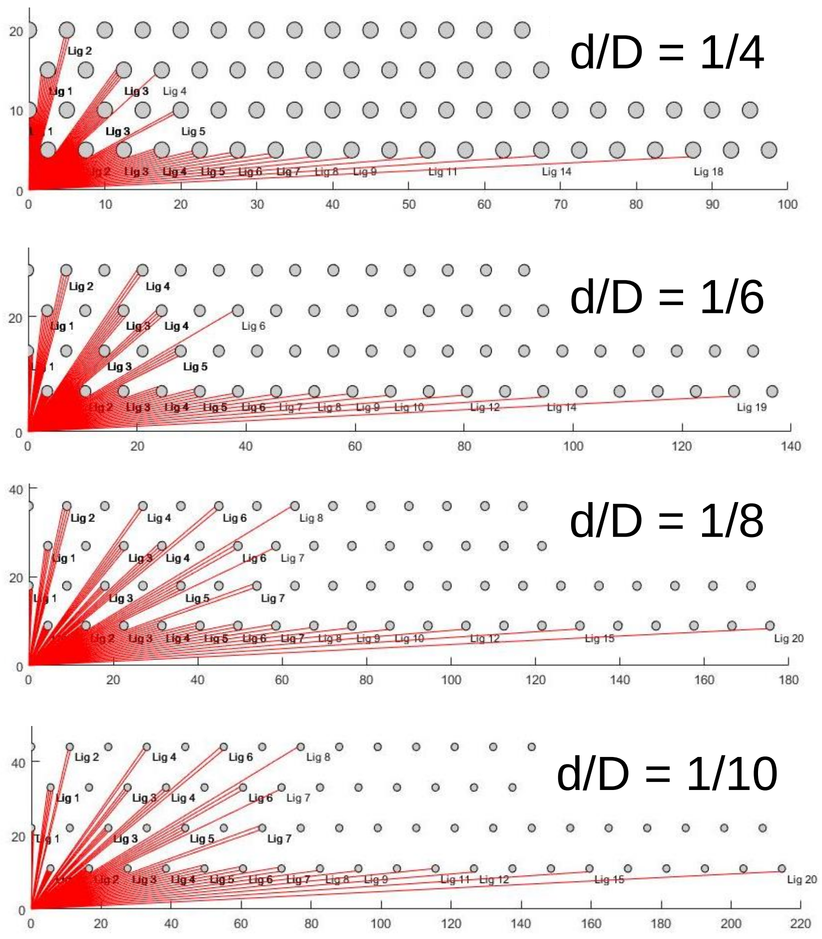

Case Study 1: 10 PPI Yield greater than 40 PPI Yield

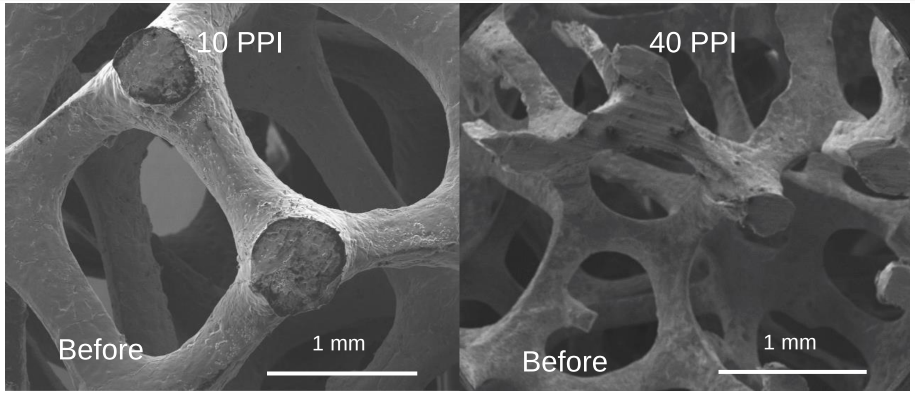

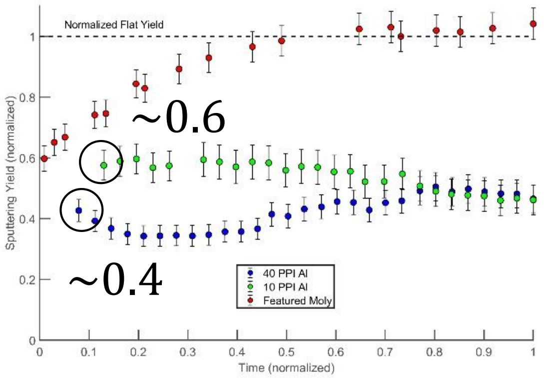

Observations:

- 10 PPI foam initially has a larger yield with 300 eV Ar^+ than 40 PPI foam
- 10 PPI has smaller pore density but thicker ligaments compared to 40 PPI
- $\xi_{10} = 3.0 > \xi_{40} = 0.7 \quad \left(\xi = \frac{D}{L_s}\right)$

Plasma-infused

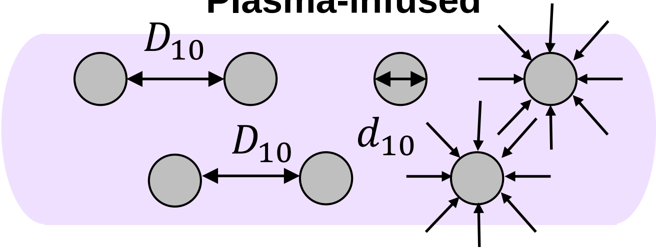

Plasma-facing

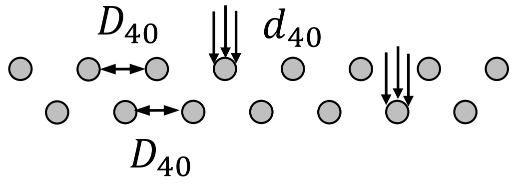

$$\frac{d_{10}}{D_{10}} \approx \frac{d_{40}}{D_{40}} \approx \frac{1}{6}$$

Same self-similar dimensions.

$$\frac{Y_{\text{eff}}}{Y_{\text{flat}}} = \underbrace{\frac{2d}{D} f_A(\xi) f_\beta(E,\xi)}_{\delta Y_1} + \underbrace{\frac{2d}{D} f_A(\xi) f_\beta(E,\xi)\left[1 - f_{dep}^{(2)}\left(\frac{d}{D}\right)\right]}_{\delta Y_2}$$

Plasma-infused

$$\frac{f_A(10\ \text{PPI}) f_\beta(10\ \text{PPI})}{f_A(10\ \text{PPI}) f_\beta(40\ \text{PPI})} \approx 2$$

Plasma-facing

Plasma-infused has larger effective sputtering area.

Case	δY_1	δY_2	$Y_{\text{eff}}/Y_{\text{flat}}$
Plasma-infused	0.52	0.25	0.77
Plasma-facing	0.28	0.13	0.41

Conclusion:

I. 10 PPI sample initially has a larger yield due to higher effective sputtering area from more plasma-infusion compared to 40 PPI foam

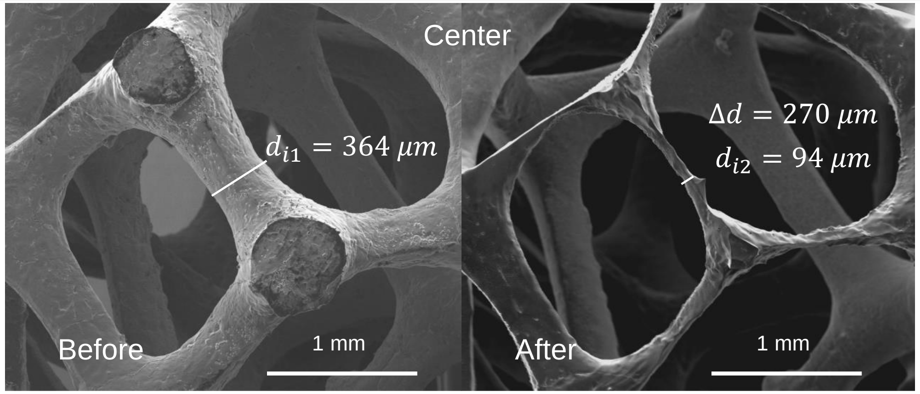

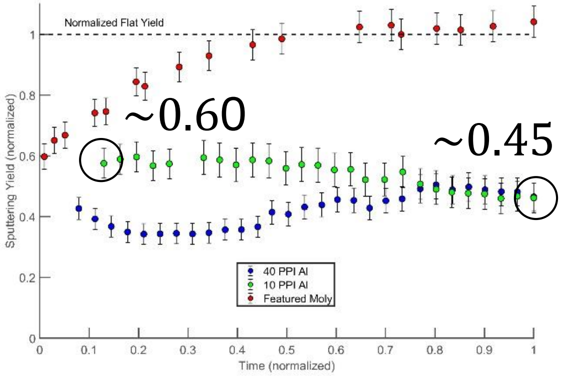

Observations:

- Thinning ligaments of 10 PPI foam from 300 eV Ar^+ lead to reduction in yield from 0.60 to 0.45
- 2nd layer relatively unchanged
- $\xi \sim 3.0$ indicates partially plasma-infused behavior

Before

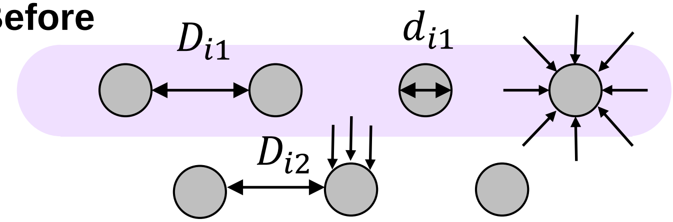

After

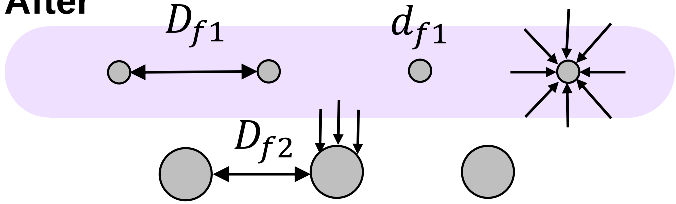

1st Layer - Plasma-infused (PI)

2nd Layer - Plasma-facing (PF)

$$\frac{Y_{\mathrm{eff}}}{Y_{\mathrm{flat}}} = \underbrace{\frac{2d_1}{D_1} f_{A1}(\xi) f_{\beta 1}(E,\xi)}_{\delta Y_1} + \underbrace{\frac{2d_2}{D_2} f_{A2}(\xi) f_{\beta 2}(E,\xi)\left[1 - f_{dep}^{(2)}\left(\frac{d_1}{D_1}\right)\right]}_{\delta Y_2}$$

Case	δY_1 (PI$_1$)	δY_2 (PF$_2$)	$Y_{\mathrm{eff}}/Y_{\mathrm{flat}}$ (PI$_1$,PF$_2$)	$Y_{\mathrm{eff}}/Y_{\mathrm{flat}}$ (PI$_1$,PI$_2$)	$Y_{\mathrm{eff}}/Y_{\mathrm{flat}}$ (PF$_1$,PF$_2$)
Before	0.45	0.12	0.57	0.77	0.36
After	0.10	0.20	0.30	0.47	0.25

Conclusions:

I. Yield for thinning ligaments decreases due to larger effect of lower opacity of 1st layer than reduced deposition

II. 10 PPI foam is in a partially-infused regime

Conclusions and Path Forward

Conclusions

- Persistent sputtering yield is possible with volumetrically complex surfaces
- Plasma-infused materials offer a unique plasma-material boundary

Path Forward

- Many explorations, including…
- Increased plasma and thermal loading
- Analysis of material property evolution
- Geometry and material optimization with fusion-relevant materials
- Opportunities for electron conduction and thermal energy transport for high-energy plasma applications
- Applications include propulsion, fusion, hypersonics, manufacturing, etc.

DOE/ARPA-E/FES GAMOW Project:

AMPERE: **A**dvanced **M**aterials for **P**lasma-**E**xposed **R**obust **E**lectrodes

AFOSR AIR FORCE OFFICE OF SCIENTIFIC RESEARCH

AFRL THE AIR FORCE RESEARCH LABORATORY LEAD I DISCOVER I DEVELOP I DELIVER

NASA

THE AEROSPACE CORPORATION

U.S. DEPARTMENT OF ENERGY